AD NUMBER
AD385284
CLASSIFICATION CHANGES
TO: **UNCLASSIFIED**
FROM: **SECRET**
LIMITATION CHANGES
TO: **Approved for public release; distribution is unlimited.**
FROM: **Distribution authorized to U.S. Gov't. agencies only; Administrative/Operational Use; NOV 1967. Other requests shall be referred to Arnold Engineering Development Center, Arnold AFB, TN.**
AUTHORITY
ASD ltr 28 Nov 1972 ; ASD ltr 16 Aug 1977

300438 AEDC-TR-67-231

300438

WIND TUNNEL INVESTIGATION OF A 1/9-SCALE BOEING COMPANY AMSA AIRPLANE-INLET MODEL AT TRANSONIC AND SUPERSONIC MACH NUMBERS (U)

D. C. Baker
ARO, Inc.

November 1967

NOTE:
PUB RELEASE,
UNLIMITED

prohibited by law.

PROPULSION WIND TUNNEL FACILITY
ARNOLD ENGINEERING DEVELOPMENT CENTER
AIR FORCE SYSTEMS COMMAND
ARNOLD AIR FORCE STATION, TENNESSEE

NOTICES

When U. S. Government drawings specifications, or other data are used for any purpose other than a definitely related Government procurement operation, the Government thereby incurs no responsibility nor any obligation whatsoever, and the fact that the Government may have formulated, furnished, or in any way supplied the said drawings, specifications, or other data, is not to be regarded by implication or otherwise, or in any manner licensing the holder or any other person or corporation, or conveying any rights or permission to manufacture, use, or sell any patented invention that may in any way be related thereto.

Qualified users may obtain copies of this report from the Defense Documentation Center.

References to named commercial products in this report are not to be considered in any sense as an endorsement of the product by the United States Air Force or the Government.

Do not return this copy. When not needed, destroy in accordance with pertinent security regulations.

AEDC-TR-67-231

WIND TUNNEL INVESTIGATION OF A 1/9-SCALE BOEING COMPANY AMSA AIRPLANE-INLET MODEL AT TRANSONIC AND SUPERSONIC MACH NUMBERS (U)

D. C. Baker

ARO, Inc.

FOREWORD

(U) The work reported herein was done at the request of the Aeronautical Systems Division (ASD), Air Force Systems Command (AFSC), for the Boeing Company, under Program Element 6340683F/139A.

(U) The results of the test were obtained by ARO, Inc. (a subsidiary of Sverdrup & Parcel and Associates, Inc.), contract operator of the Arnold Engineering Development Center (AEDC), AFSC, Arnold Air Force Station, Tennessee, under Contract AF40(600)-1200. The test was conducted from June 19 to August 4, 1967, under ARO Project No. PT0743, and the manuscript was submitted for publication on October 2, 1967.

(U) This report contains no classified information extracted from other classified documents.

(U) This technical report has been reviewed and is approved.

Richard W. Bradley
Lt Col, USAF
AF Representative, PWT
Directorate of Test

Leonard T. Glaser
Colonel, USAF
Director of Test

Unclassified

[redacted] ABSTRACT

(U) Test results are presented for a 1/9-scale inlet model of the AMSA air induction system at free-stream Mach numbers from 0.6 to 2.3. Inlet performance was determined for various inlet locations and is presented as a function of free-stream Mach number, inlet mass-flow ratio, angle of attack, angle of yaw, and bypass flow rate.

CONTENTS

APPENDIX
Illustrations

NOMENCLATURE

BL	Airplane buttock line, in.
B/P	Inlet bypass door opening, percent of full open
BS	Airplane body station, in.
C/B	Inlet centerbody
D_2	Compressor-face total-pressure distortion, $(p_{t2})_{max} - (p_{t2})_{min}/(p_{t2})_{avg}$
IS	Inlet station, in.
M_∞	Free-stream Mach number
m_2/m_0	Inlet mass-flow ratio, ratio of compressor-face mass flow to inlet capture mass flow
N_2	Compressor-face total-pressure recovery $(p_{t2})_{avg}/p_{t_\infty}$
p_{t2}	Compressor-face local total pressure, psf
p_{t_∞}	Free-stream total pressure, psf
WL	Airplane waterline, in.
α	Model angle of attack, deg
ψ	Model angle of yaw, positive nose right, deg

SECTION I
INTRODUCTION

(U) The Advanced Manned Strategic Aircraft (AMSA) is under development as a manned weapon system with long range and large load carrying capability. A series of alternative configuration requirements have been investigated with all configurations being designed for the primary mission of penetrating at low altitude from the enemy's warning line to the target and exit at subsonic (Mach 0.85) speeds. The configuration requirements include a design capable of subsonic low altitude and Mach 2.2 high altitude operation. The AMSA will utilize variable geometry wings to provide optimum flight characteristics for both low and high altitude flight.

(U) A 1/9-scale model of the AMSA was tested in the Propulsion Wind Tunnel, Transonic (16T) and Propulsion Wind Tunnel, Supersonic (16S) of the Propulsion Wind Tunnel Facility (PWT). The test vehicle consisted of an airplane model and two pressure-instrumented inlet nacelles.

(U) Airplane model variations representing three-engine and four-engine configurations were tested with the two engine nacelles representing either two-thirds or one-half of the full airplane configuration. The three-engine configuration consisted of one pylon-mounted nacelle under the left wing and one tail-mounted nacelle above the fuselage on the airplane vertical centerline. The symmetrical four-engine configurations had either two adjacent nacelles suspended under the left wing or one forward nacelle under the left wing and one nacelle mounted aft on the left side of the fuselage near the tail.

(U) Data were obtained at free-stream Mach numbers from 0.60 to 2.30 to determine the performance characteristics of the inlets, and the effects of mutual interactions of inlets and airplane surfaces. The model attitude was varied throughout an angle-of-attack range of -4 to +11 deg and yaw angles of ±4 deg.

SECTION II
APPARATUS

2.1 TEST FACILITIES

(U) Tunnel 16T is a closed-circuit, continuous flow wind tunnel that can be operated at Mach numbers from 0.55 to 1.60. The tunnel

can be operated over a stagnation pressure range from approximately 160 to 4000 psfa and over a stagnation temperature range from 80 to 160°F. The tunnel specific humidity is controlled by removing tunnel air and supplying conditioned makeup air from an atmospheric dryer. Perforated walls in the test section allow continuous operation through the Mach number range with a minimum of wall interference.

(U) Tunnel 16S is a closed-circuit, continuous flow wind tunnel that can be operated at Mach numbers from 1.65 to 3.20. The tunnel can be operated over a stagnation pressure range from 100 to approximately 1600 psfa. The test section stagnation temperature can be controlled through the range of 100 to 650°F. The tunnel specific humidity is controlled by removing tunnel air and supplying conditioned makeup air from an atmospheric dryer.

(U) Details of the test sections showing the model location and the sting support arrangement are presented in Figs. 1 and 2. A more extensive description of each tunnel and its operating characteristics is contained in the Test Facilities Handbook.[1]

2.2 TEST ARTICLE

2.2.1 Airplane Model

(S) The model was a 1/9-scale general configuration of the basic AMSA airplane with the variable swept wings in the full-retracted position. The wing tips, aft of the aft inlet cowl lip station, and horizontal stabilizer were removed to reduce aerodynamic loads on the wind tunnel model. Photographs of the three basic model configurations investigated are shown in Fig. 3.

2.2.2 Inlet Nacelles

(S) The two identical inlet nacelle models simulate an axisymmetric, mixed compression, variable diameter centerbody inlet with centerbody supporting struts. Four interchangeable, fixed-geometry centerbodies were provided. The centerbody contours were selected to provide inlet contraction ratios for high inlet performance at nominal Mach numbers of 1.60, 1.80, 2.20, and 2.35. The centerbodies were remotely translatable to facilitate inlet starting, and had boundary-layer

[1]Test Facilities Handbook (6th Edition). "Propulsion Wind Tunnel Facility, Vol. 5." Arnold Engineering Development Center, November 1966.

bleed flow provisions. The fixed-geometry cowl also had provisions for boundary-layer bleed flow. Both the cowl and centerbodies had vortex generators with the exception of the 1.6 centerbody which had too small a diameter to allow satisfactory installation of the vortex assemblies. Engine bypass flow was removed through perforations in the cowl inner surface immediately in front of the compressor-face station. A calibrated flow tube for measuring engine mass flow and a remotely controlled exhaust nozzle plug valve for varying the engine mass flow were provided in each inlet nacelle model. A cross-sectional view of the inlet nacelle, including tables of cowl and centerbody contours, is shown in Fig. 4.

(U) The various inlet locations on the airplane model are shown in Fig. 5. All model stations locating the inlets are given for the inlet cowl lip centerline. The two-inlet under-wing configuration was tested with and without splitter plates. The installation of the inlets and splitter plates is shown in Fig. 6, and a sketch of the primary inlet-splitter plate configuration is shown in Fig. 7.

2.3 INSTRUMENTATION

(U) Inlet performance in terms of total-pressure recovery and flow distortion were obtained from total-pressure rakes located at the compressor face. The compressor-face pressure orifices were located on centers of equal areas as shown in Fig. 8. Two model-mounted dynamic transducers also located at the compressor face were monitored on oscilloscopes to determine inlet stability. Total-pressure measurements from a sixteen-tube total-pressure rake located in a calibrated flow tube were used to calculate compressor-face mass flow. The locations of the flow tube orifices are shown in Fig. 9.

SECTION III
PROCEDURE

(U) After the tunnel free-stream total pressure and Mach number were established, the model was positioned to the desired angle of attack and/or yaw angle. At each test Mach number and model attitude the optimum inlet setting (maximum compressor-face total-pressure recovery) was determined by closing the remotely controlled plug valve until the inlet unstarted. Inlet unstarts were detected by monitoring both compressor-face dynamic pressure and a twenty-tube compressor-face pressure averager which displayed average compressor-face total pressure versus plug position on an x-y plotter.

(U) Inlet restarts with the fixed-geometry centerbodies were accomplished by both opening the plug valve and translating the centerbody forward to increase the minimum inlet throat area.

(U) After determining the optimum inlet setting, steady-state pressure data were obtained for both optimum and supercritical settings of the plug valve. (A steady-state data point was also obtained just after inlet unstart when applicable.)

SECTION IV
RESULTS AND DISCUSSION

(U) Inlet performance in terms of compressor-face total-pressure recovery (N_2) and distortion (D_2) is presented as a function of free-stream Mach number, inlet mass-flow ratio, angle of attack, angle of yaw, and bypass flow. With the exception of inlet performance as a function of mass-flow ratio and inlet unstart conditions, all data are presented for the maximum inlet recovery at the Mach number and inlet setting indicated.

(U) The predicted cruise attitude of the AMSA model as discussed in this report is defined as follows: At free-stream Mach numbers up to and including Mach number 1.60, the cruise attitude is assumed to be +3-deg angle of attack and 0-deg angle of yaw; at free-stream Mach numbers greater than 1.60, the cruise attitude is assumed to be +5-deg angle of attack and 0-deg angle of yaw.

4.1 INLET PERFORMANCE

(U) Inlet performance data are presented in Fig. 10 for the five basic inlet locations investigated. The inlet at location VI was investigated only briefly and will be discussed later in the report under Section 4.2. The various inlet locations, shown in Fig. 5, were investigated in pairs as shown in Fig. 3. At the various inlet locations, fixed-geometry centerbodies representing different operating points of a variable-diameter centerbody inlet were investigated to determine inlet performance as a function of free-stream Mach number. As shown in Fig. 10, for a given centerbody, the compressor-face total-pressure recovery decreased at all inlet locations as the free-stream Mach number was increased. This decrease in inlet recovery would be expected, because, as the free-stream Mach number increases the losses across the inlet shock system are greater. The unstart Mach number for each

centerbody and for each inlet location was not precisely defined during this test; however, the maximum compressor-face total-pressure recovery shown in Fig. 10, for the 2.20 and 2.35 centerbodies, was obtained at a free-stream Mach number within 0.1 Mach number of unstart. Comparison of the recovery data at the various inlet locations with the 2.20 centerbody installed, shows that the maximum compressor-face total-pressure recovery (93 percent) was obtained with the inlet pylon mounted under the wing (inlet location I). The maximum recovery obtained at inlet location I was 2.5 percent greater than the maximum recovery obtained for the tail-mounted inlet (inlet location II) with the 2.2 centerbody installed. Comparison of the data at various inlet locations with the 1.60 centerbody, representing the fully collapsed position of the variable geometry centerbody, shows that better recovery was obtained at all Mach numbers investigated with the inlet either pylon mounted or installed under the wing (inlet locations I, IV, and V) compared to the tail-mounted inlets (inlet locations II and III). These variations in inlet performance at the various inlet locations represent the effects of the local Mach number and local flow disturbances associated with inlet location.

(U) As shown in Fig. 10, the variation of compressor-face total-pressure distortion with free-stream Mach number showed the same trend for all inlet locations with the distortion varying from approximately 0.15 at Mach number 2.30 to approximately 0.05 at Mach number 0.60. The tail-mounted configurations (inlet locations II and III), however, had noticeably higher distortion levels at Mach number 1.40 than the other inlet locations investigated.

4.1.1 Inlet Mass-Flow Ratio

(U) Inlet performance is presented in Fig. 11 as a function of inlet mass-flow ratios for inlet locations I through V. These data represent typical model cruise performance for a given centerbody at selected free-stream Mach numbers; however, for the 2.20 and 2.35 centerbodies the data are presented at a free-stream Mach number close to the unstart conditions of the inlet for each respective centerbody. Intentional inlet unstarts were obtained at the higher Mach numbers (1.80 and above) and were accompanied by a large decrease in recovery and, in general, an increase in distortion, as shown by the solid symbols in Fig. 11. At the higher Mach numbers, with the inlet operating at the Mach number close to unstart for the respective centerbody, operating the inlet supercritical resulted in an abrupt decrease in compressor-face total-pressure recovery and an increase in distortion.

4.1.2 Angle of Attack

(S) The effect of angle of attack on inlet performance at 0-deg yaw angle is presented in Fig. 12 for inlets at locations I through V. In general, for all inlet locations, the maximum compressor-face total-pressure recovery and minimum distortion occurred at or close to the cruise angle of attack for a given centerbody and free-stream Mach number, indicating good inlet alignment with the local flow direction. It should also be noted that small changes in angle of attack near the cruise attitude of the airplane had little effect on the inlet performance at all inlet locations. At the higher Mach numbers (M_∞ = 1.80 and above), however, the angle-of-attack range was restricted by inlet unstarts to within the limits shown by the dashed lines in Fig. 12. As mentioned previously, the unstart Mach number for a given centerbody was not determined precisely; therefore, these data do not necessarily represent the angle-of-attack limits of the inlet operating at maximum performance.

4.1.3 Angle of Yaw

(S) The effect of angle of yaw on inlet performance at the cruise angle of attack is presented in Fig. 13 for inlets at locations I through V. In general, for all inlet locations, the maximum compressor-face total-pressure recovery and the minimum distortion occurred at or near zero-deg yaw angle for a given centerbody and free-stream Mach number, indicating good inlet alignment in the yaw plane with local flow direction. At the higher Mach numbers (M_∞ = 1.80 and above), the angle-of-yaw range was restricted by inlet unstarts to within the limits shown by the dashed lines in Fig. 13. From a comparison of the angle-of-yaw and the angle-of-attack data, at a given inlet location, it is apparent that the inlet performance is affected more by small changes in yaw angle than for the same change in angle of attack. Again it should be noted that the yaw limits do not necessarily represent the limits of the inlet operating at maximum performance.

4.1.4 Bypass Flow

(S) The effect of bypass flow on inlet performance at the model cruise attitude is presented in Fig. 14 for inlets at locations I through V. The data indicate that, for all inlet locations, with the 2.2 centerbody operating near the unstart Mach number, good control of the bypass flow was available with essentially no loss in inlet performance. At lower free-stream Mach numbers (M_∞ = 1.20 and below), however, the pressure drop across the bypass system was inadequate, resulting in only small changes in inlet mass-flow ratios for bypass door openings up to 80 percent of full open.

4.2 MUTUAL INLET INTERACTION

(U) The two-inlet, under-wing configuration was tested with various combinations of splitter plates, splitter plate locations, and inlet locations. The under-wing model configuration with inlets at locations IV and VI and no splitter plate installed was tested initially. With this installation an intentional unstart of either the inboard or outboard inlet caused the adjacent inlet to unstart. A short splitter plate, shown in Figs. 6b and 7, was then installed, but there was no improvement in inlet unstart interactions. The short splitter plate was then replaced with a long splitter plate shown in Fig. 6c. With this installation there was no interaction between inlets when either inlet unstarted; however, the inlet performance was degraded at some model attitudes because of the forward extension of the splitter plate.

(U) The inboard inlet was then moved farther inboard resulting in inlet location V. With the short splitter plate installed between the inlets and the inlets at locations IV and V, as shown in Fig. 7, there was no interaction between either the two adjacent inlets or between splitter plate and inlet.

SECTION III
CONCLUSIONS

(U) Based on the results of this investigation of a 1/9-scale AMSA, the following conclusions were reached:

(U) 1. Inlet performance was affected by the local flow conditions at the various inlet locations. In general, better inlet performance was obtained at the pylon and under-wing inlet locations (inlet locations I, IV, and V) than at the tail-mounted locations (inlet locations II and III).

(U) 2. In general, maximum inlet performance occurred at predicted airplane cruise attitude for all inlet locations.

(U) 3. At the higher free-stream Mach numbers, good bypass flow control was available with little effect on inlet performance.

(U) 4. The two-inlet, under-wing configuration with inlet locations IV and V had no mutual inlet interaction with a splitter plate installed between the inlets.

APPENDIX
ILLUSTRATIONS

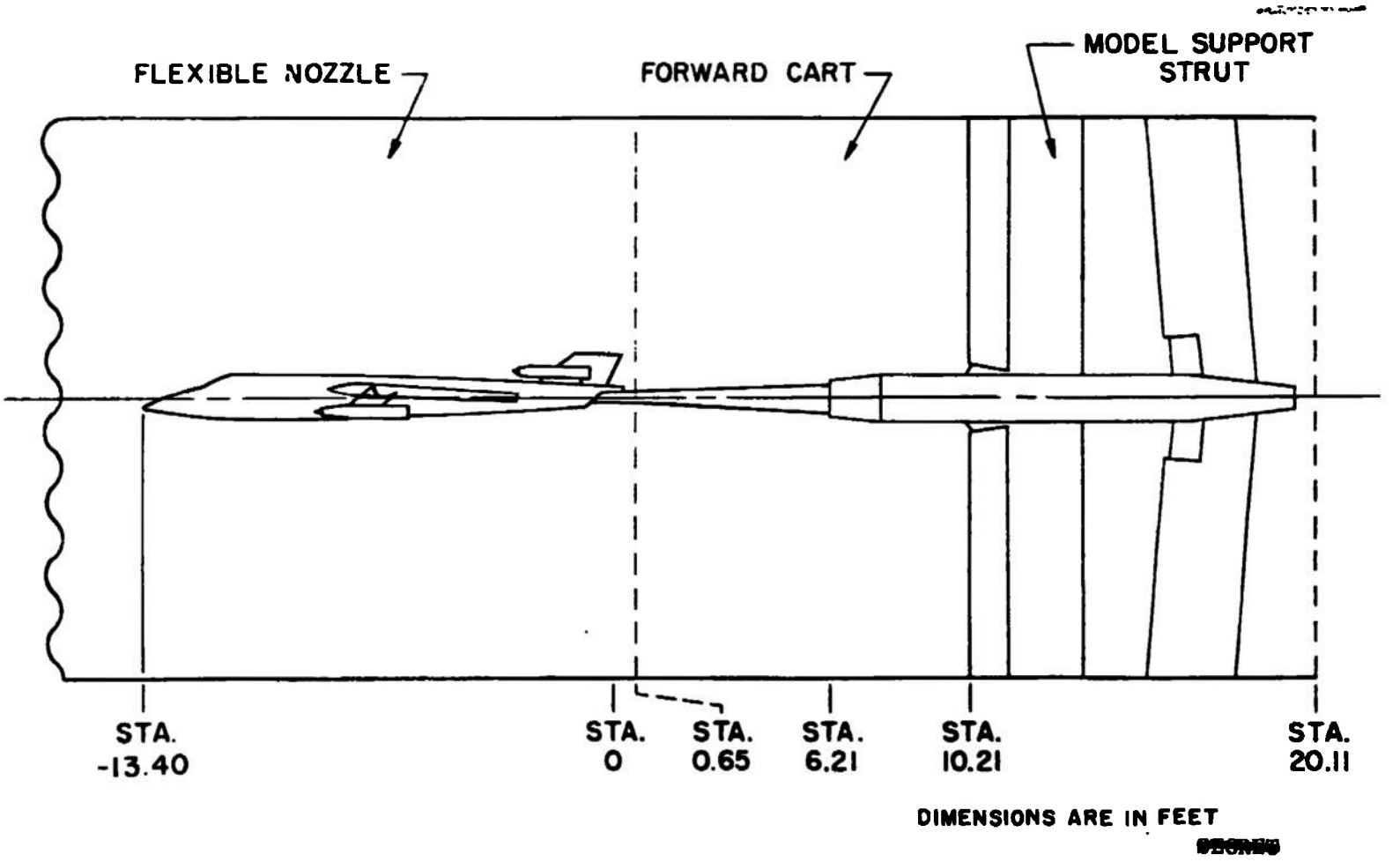

Fig. 1 Location of the AMSA 1/9-Scale Model in Tunnel 16S

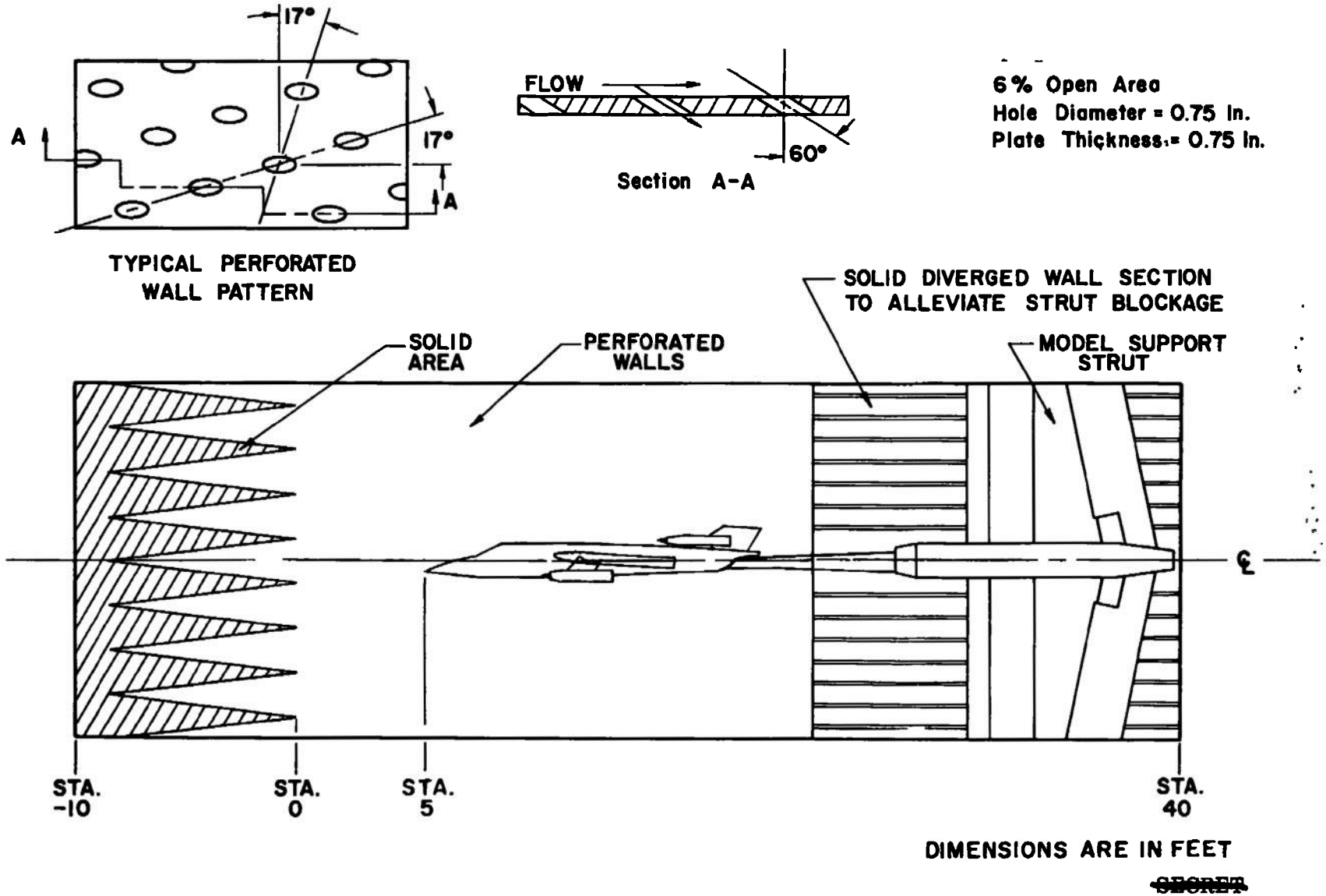

Fig. 2 Location of the AMSA 1/9-Scale Model in Tunnel 16T

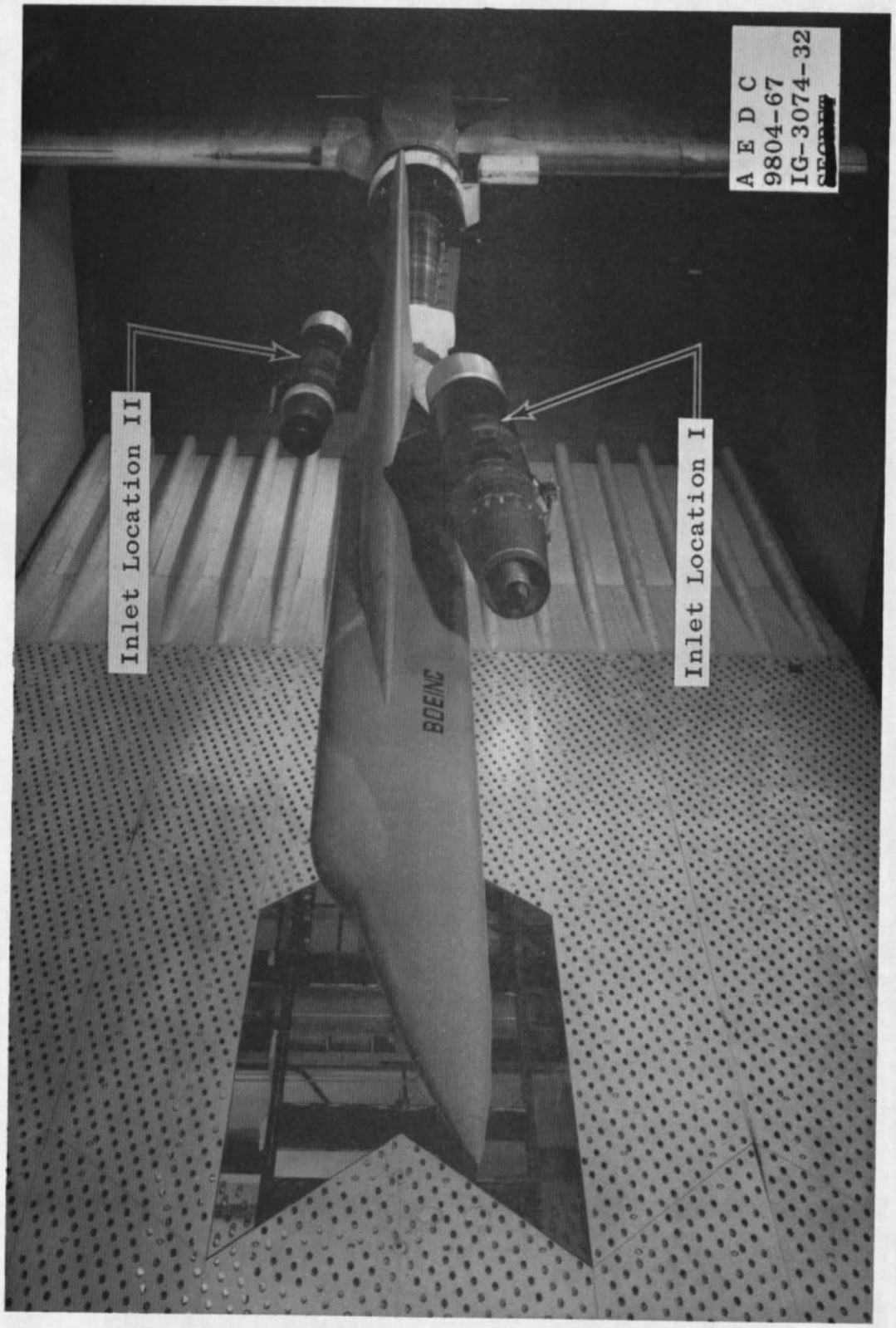

a. Inlet Locations I and II

Fig. 3 AMSA 1/9-Scale Model Installation

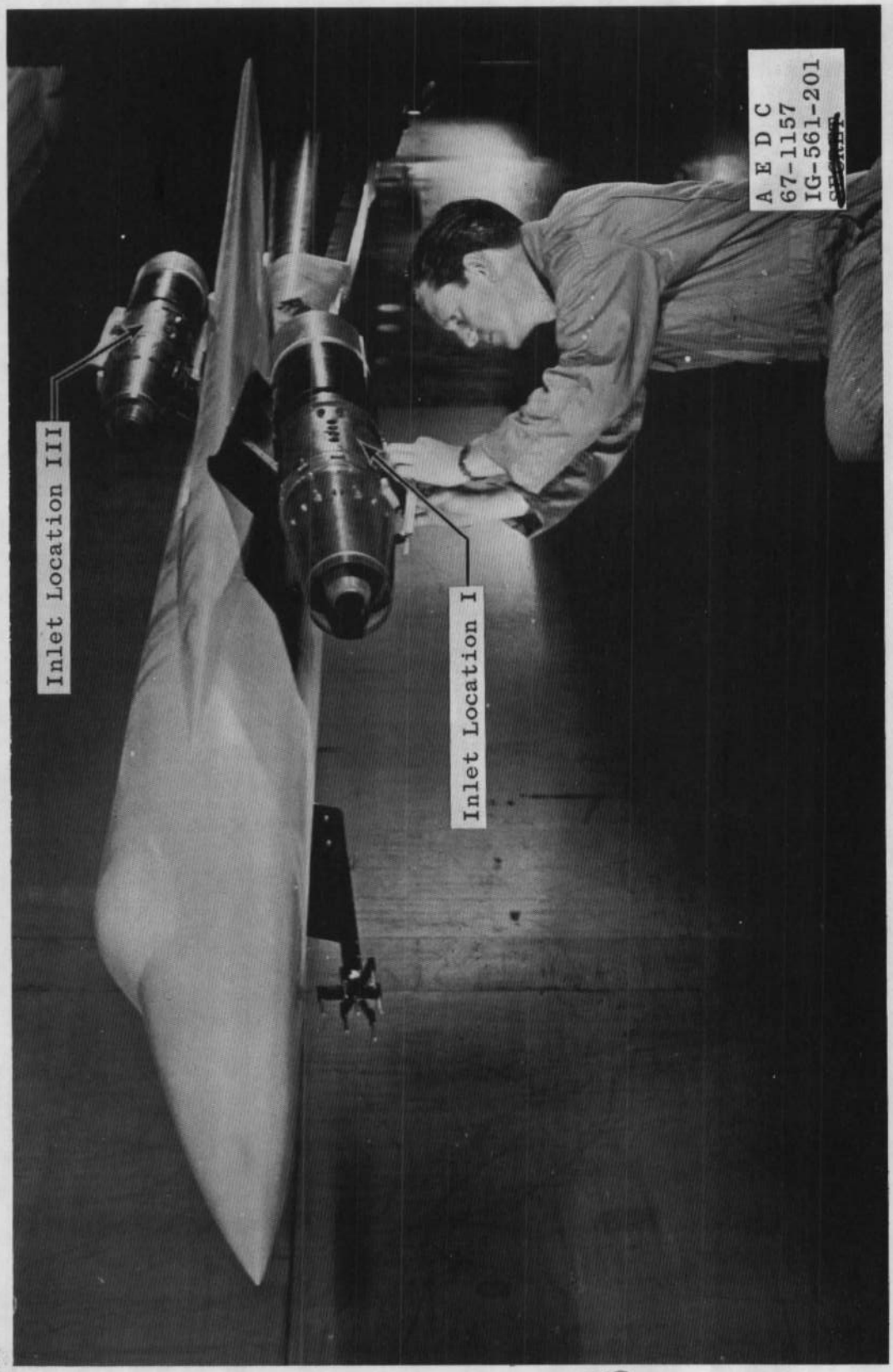

b. Inlet Locations I and III

Fig. 3 Continued

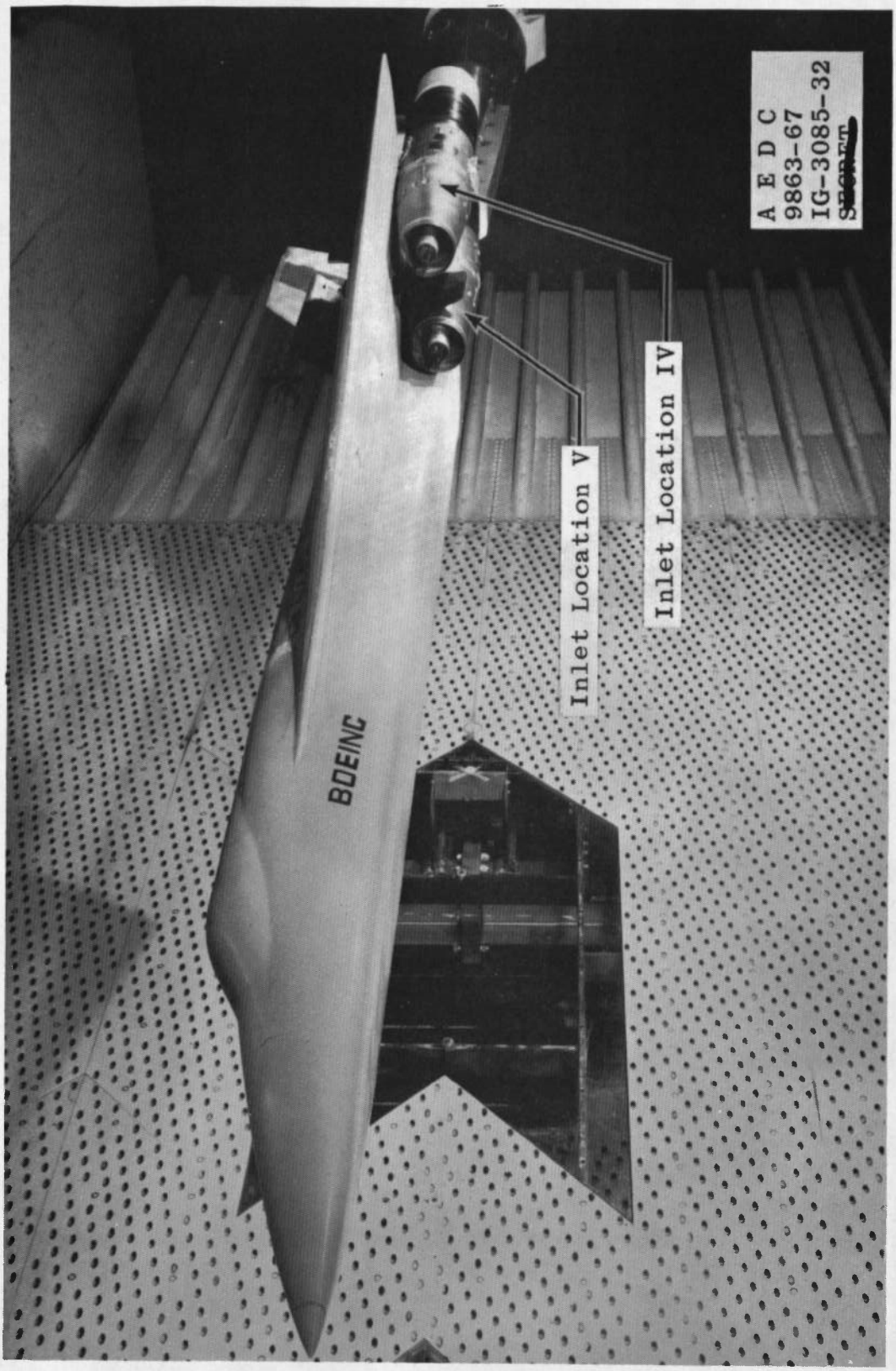

c. Inlet Locations IV and V

Fig. 3 Concluded

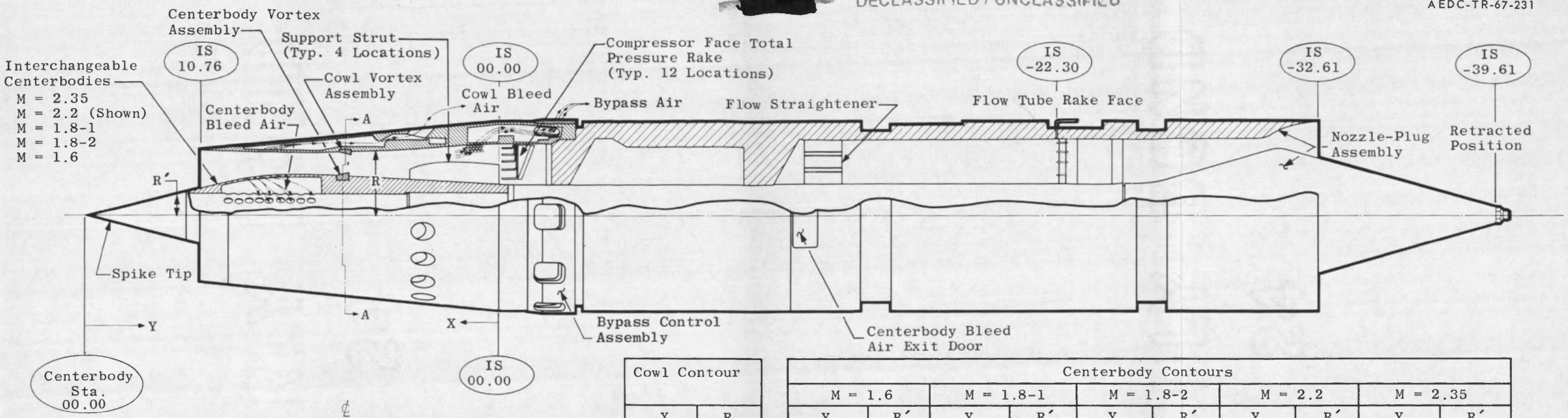

Dimensions are in inches.

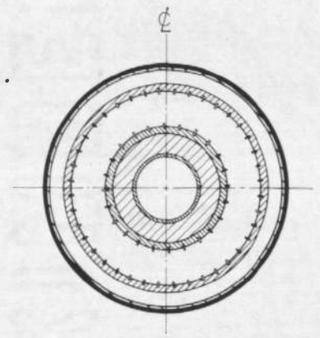

Section A-A

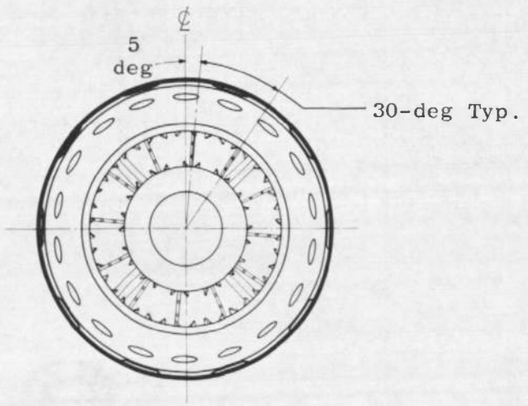

Front View

Cowl Contour	
X	R
0.000	2.796
0.130	2.788
0.258	2.780
0.773	2.744
1.285	2.709
1.799	2.675
2.312	2.640
2.569	2.623
3.083	2.589
3.596	2.563
4.110	2.542
4.624	2.526
5.137	2.512
5.651	2.502
6.164	2.493
6.421	2.491
7.280	2.491
7.370	2.491
7.637	2.493
7.905	2.497
8.172	2.503
8.540	2.510
8.707	2.519
9.075	2.529
9.342	2.540
9.510	2.549
9.777	2.556
10.045	2.562
10.312	2.565
10.558	2.568
10.758	2.568

Centerbody Contours									
M = 1.6		M = 1.8-1		M = 1.8-2		M = 2.2		M = 2.35	
Y	R′	Y	R′	Y	R′	Y	R′	Y	R′
+0.000	0.000	+0.000	0.000	+0.000	0.000	+0.000	0.000	+0.000	0.000
*3.852	0.925	*4.000	0.960	*4.000	0.960	*5.430	1.304	*6.581	1.580
4.108	0.980	4.100	0.984	4.200	1.007	5.514	1.323	6.698	1.607
4.365	1.022	4.300	1.023	4.400	1.042	5.683	1.361	6.816	1.632
4.622	1.052	4.500	1.057	4.600	1.071	5.851	1.396	6.934	1.656
4.879	1.066	4.700	1.083	+4.800	1.093	6.020	1.428	7.051	1.677
5.283	1.076	4.900	1.106	*5.454	1.156	6.189	1.458	7.169	1.697
+5.468	1.079	+5.000	1.116	5.627	1.171	6.357	1.484	7.287	1.715
*5.560	1.079	*5.716	1.187	5.799	1.183	6.526	1.508	7.404	1.730
5.744	1.078	5.871	1.201	5.971	1.193	6.695	1.530	7.522	1.744
5.927	1.074	6.026	1.213	6.137	1.200	6.864	1.548	7.639	1.756
6.110	1.066	6.180	1.222	6.313	1.204	7.032	1.564	7.757	1.767
6.292	1.056	6.334	1.229	6.484	1.206	7.201	1.578	7.875	1.775
6.474	1.044	6.488	1.234	+6.600	1.207	7.370	1.588	7.992	1.781
6.654	1.028	6.641	1.236	*9.033	1.207	7.538	1.596	8.110	1.786
6.830	1.010	6.700	1.237	9.290	1.206	7.707	1.601	8.228	1.789
7.036	0.955	7.933	1.249	9.803	1.197	7.791	1.603	+8.345	1.790
7.241	0.986	+8.088	1.251	10.060	1.189	+7.876	1.604	*9.244	1.790
7.447	0.980	*9.036	1.251	10.317	1.179	*9.244	1.604	9.501	1.786
7.549	0.977	9.293	1.250	10.700	1.161	9.758	1.595	9.758	1.781
7.733	0.980	9.806	1.241	10.800	1.159	10.271	1.576	10.014	1.773
+7.913	0.983	10.320	1.221	10.900	1.158	10.528	1.563	10.271	1.763
*9.031	0.983	10.700	1.201	11.100	1.161	10.785	1.551	10.528	1.751
9.287	0.982	10.800	1.197	15.800	1.281	15.663	1.297	10.785	1.730
10.058	0.967	+11.000	1.195	15.900	1.282	15.792	1.292	+11.041	1.709
10.314	0.957	*15.800	1.280	16.000	1.283	15.920	1.287	*15.920	1.306
10.571	0.946	15.900	1.282	+16.100	1.284	16.049	1.285	16.049	1.298
10.828	0.939	16.000	1.283	*16.485	1.284	+16.177	1.284	16.177	1.292
10.956	0.943	+16.100	1.284			*16.434	1.284	16.305	1.287
+11.085	0.951	*16.490	1.284					+16.434	1.284
*15.663	1.265							*16.742	1.284
15.792	1.272								
15.920	1.278								
16.049	1.282		Note: Straight-Line Segment Between						
+16.177	1.284		Stations Marked + *						
*16.471	1.284								

Fig. 4 Cross-Sectional View of the Inlet

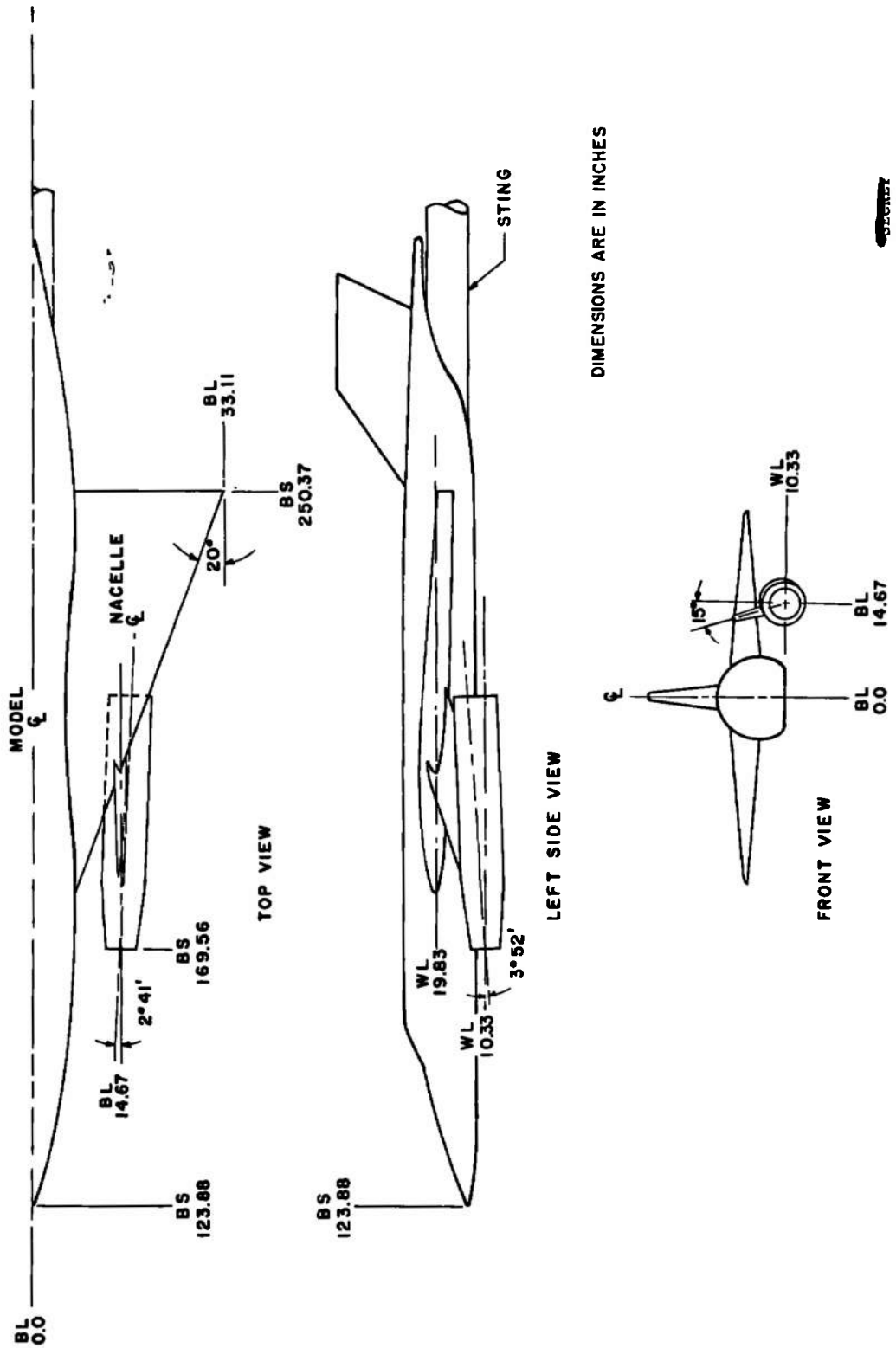

a. Inlet Location I

Fig. 5 Inlet Locations

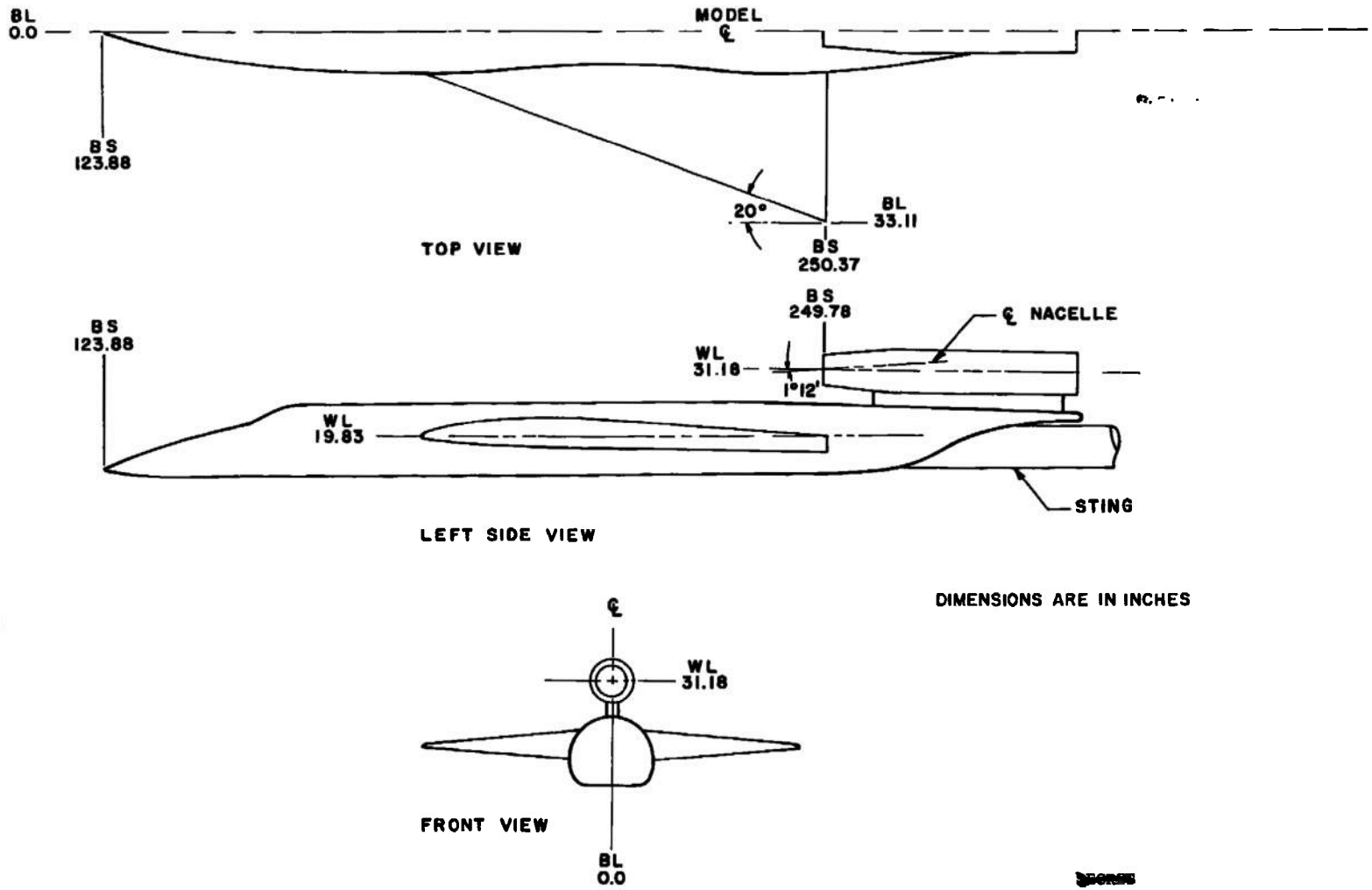

b. Inlet Location II

Fig. 5 Continued

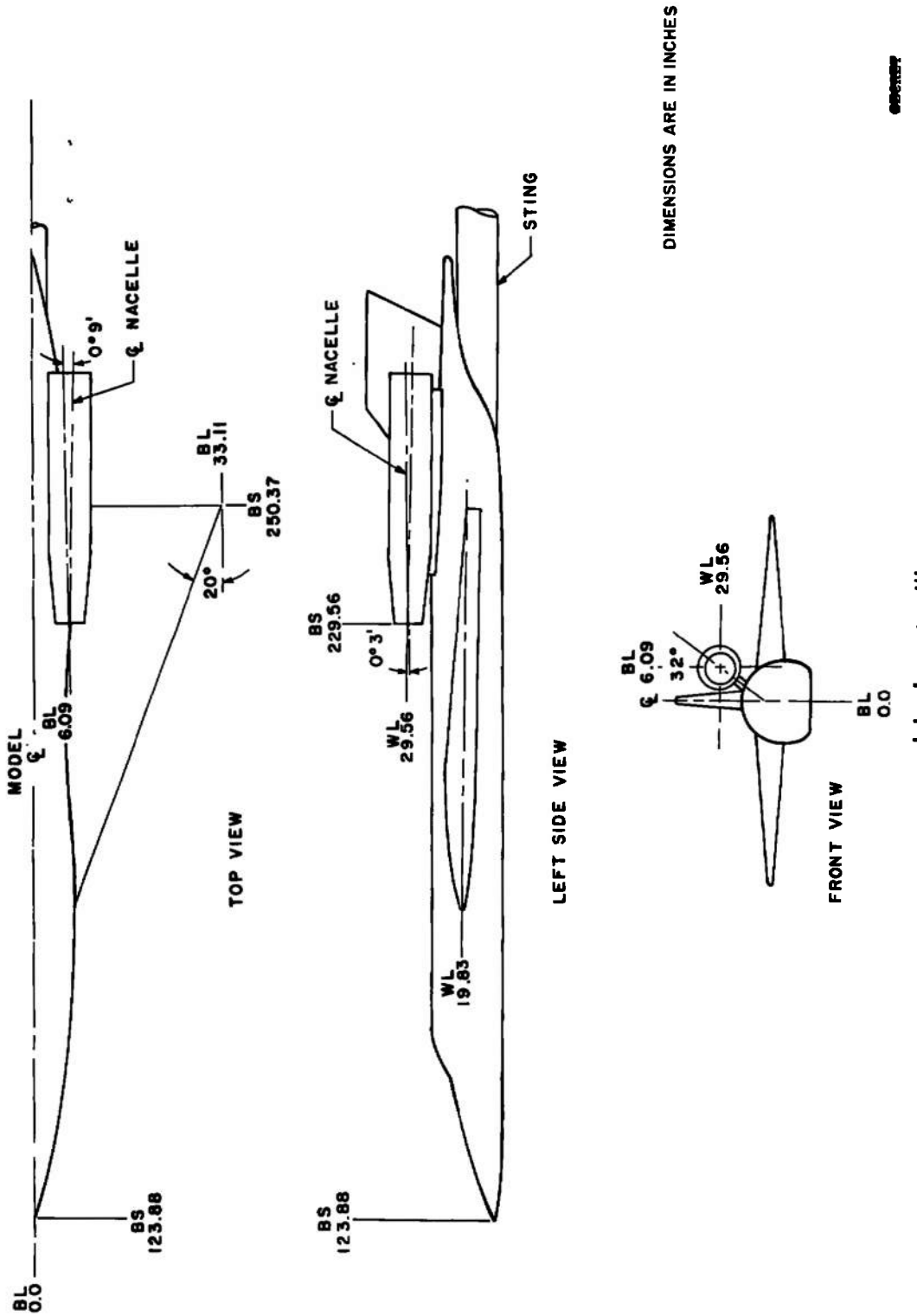

c. Inlet Location III

Fig. 5 Continued

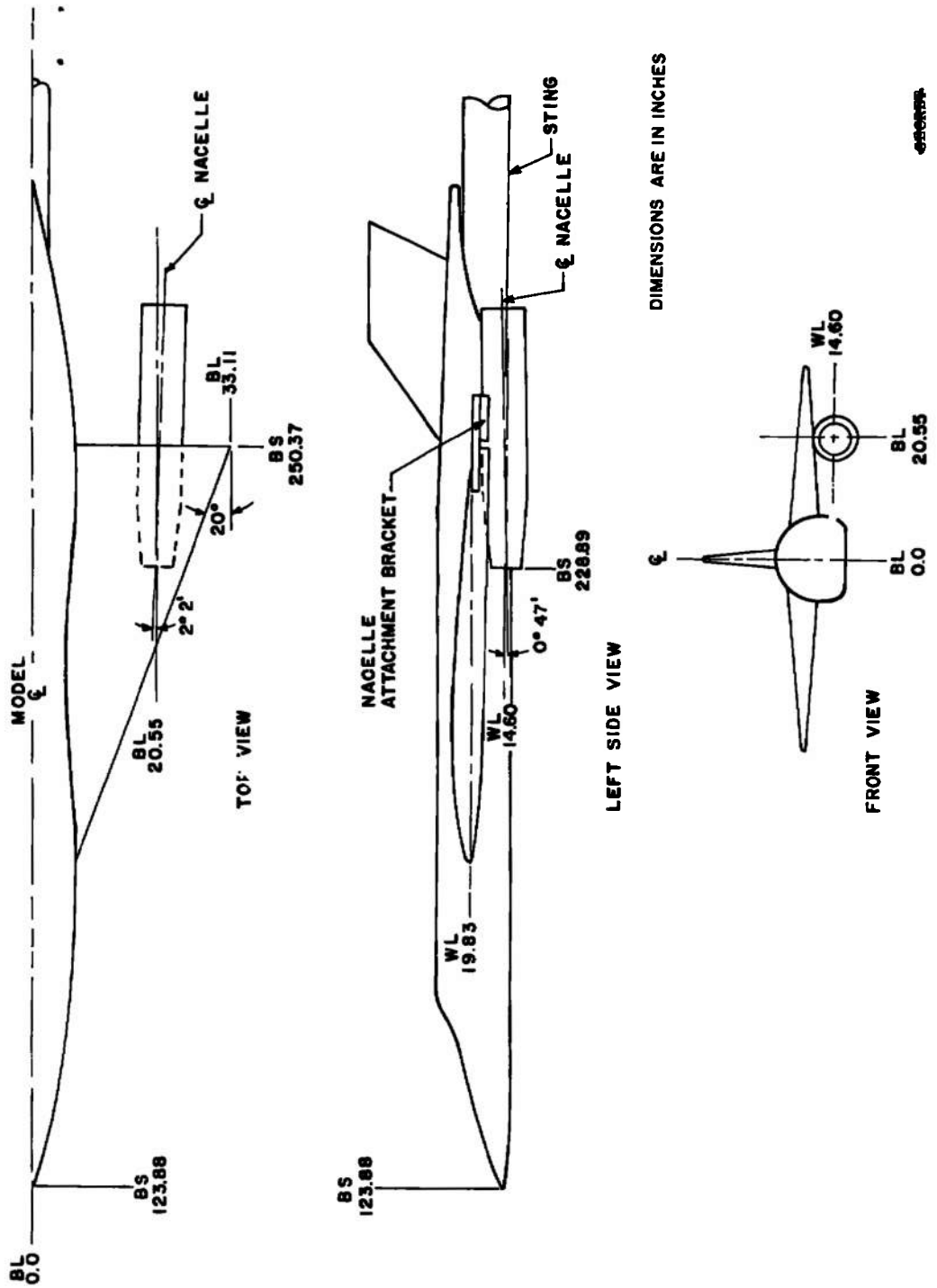

d. Inlet Location IV

Fig. 5 Continued

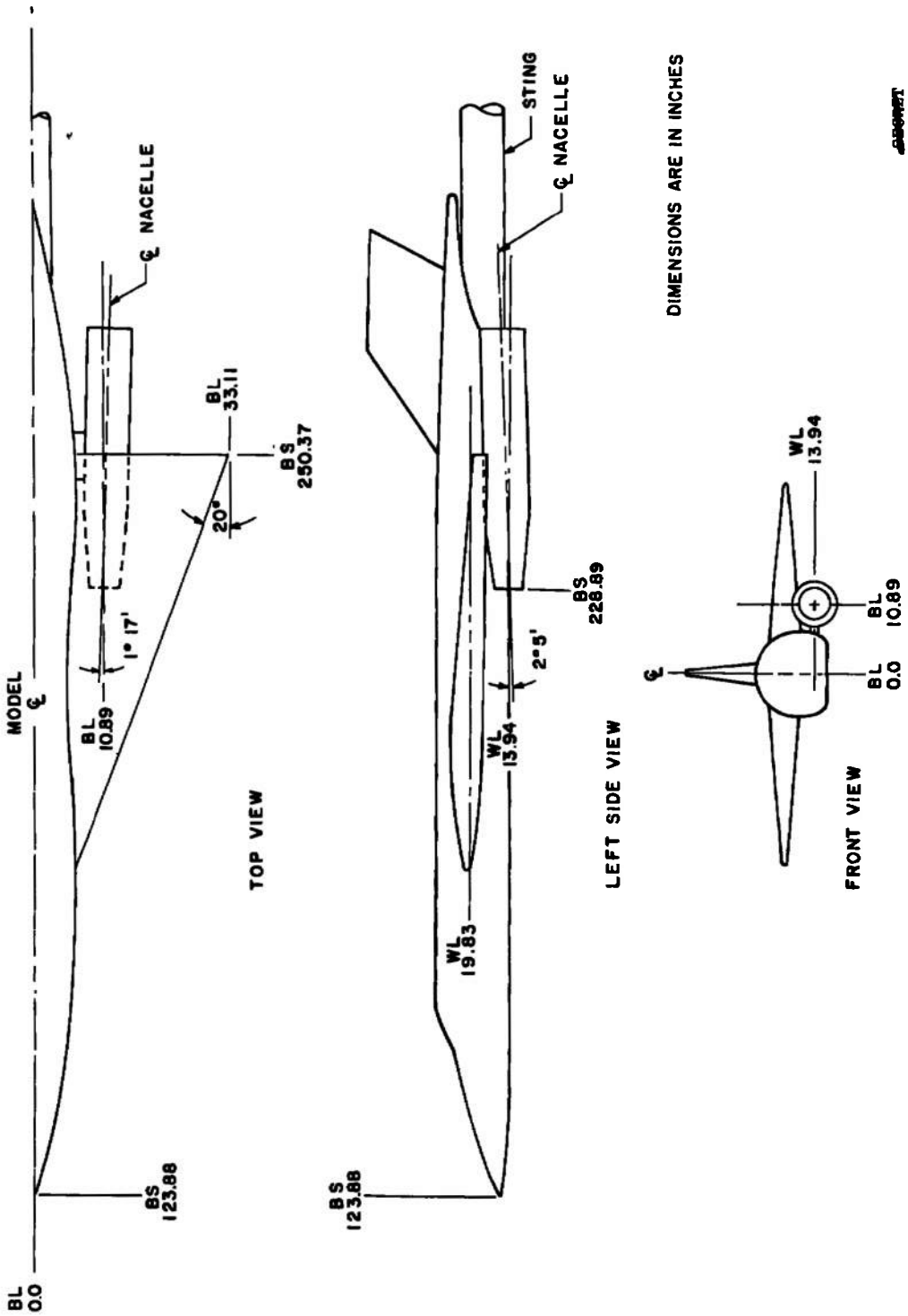

e. Inlet Location V

Fig. 5 Continued

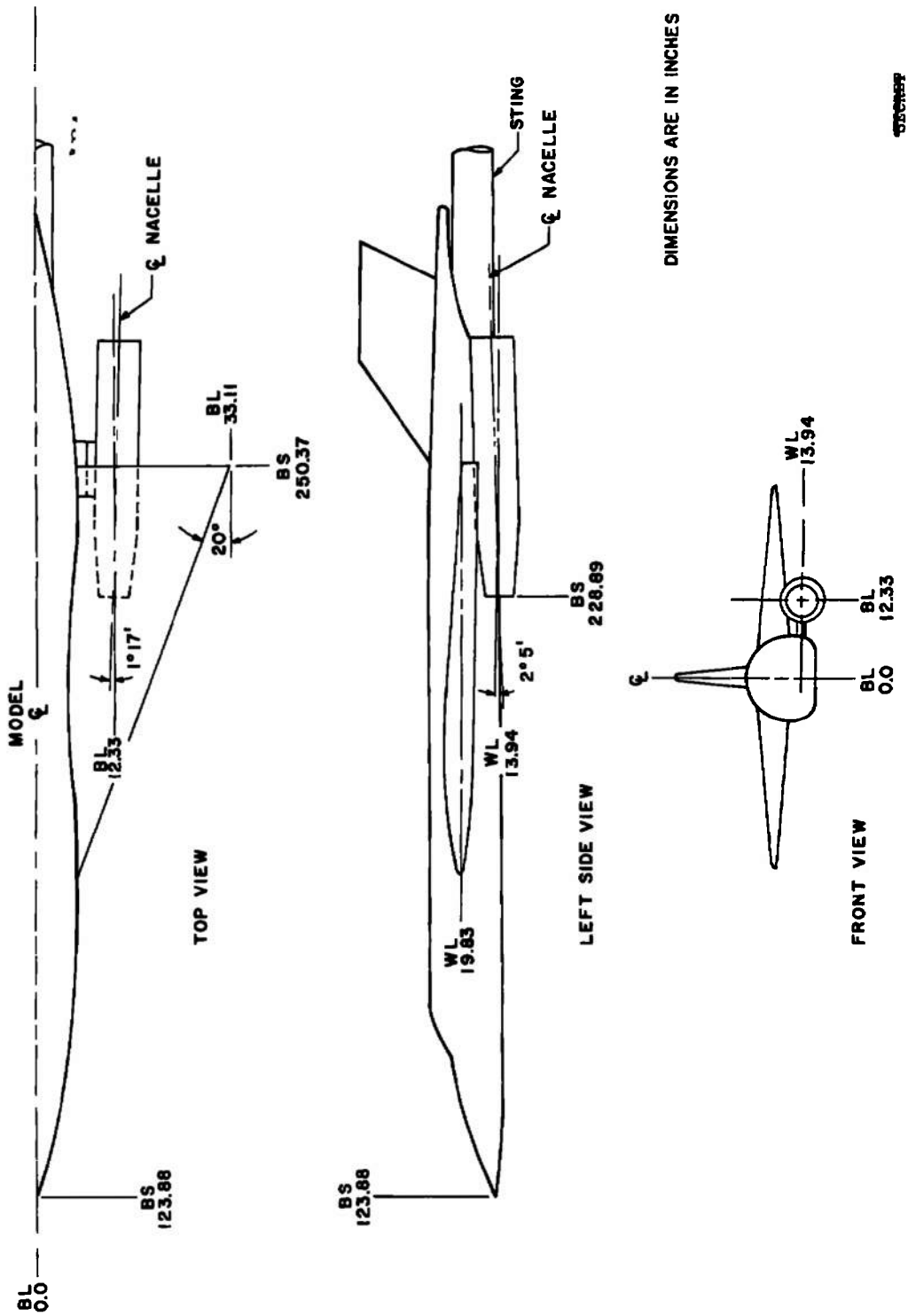

f. Inlet Location VI

Fig. 5 Concluded

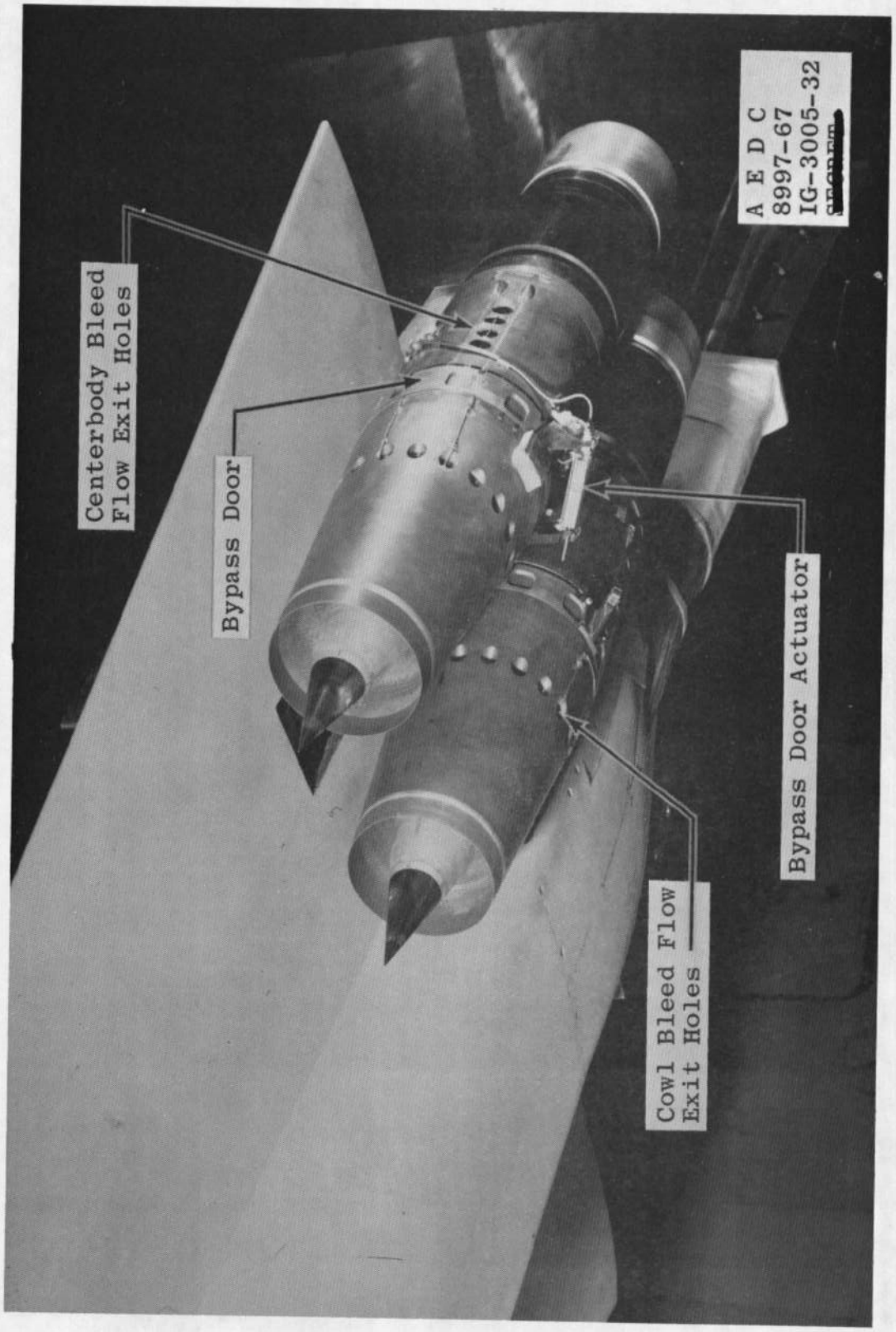

a. No Splitter Plate

Fig. 6 Two-Inlet Under-Wing Configuration

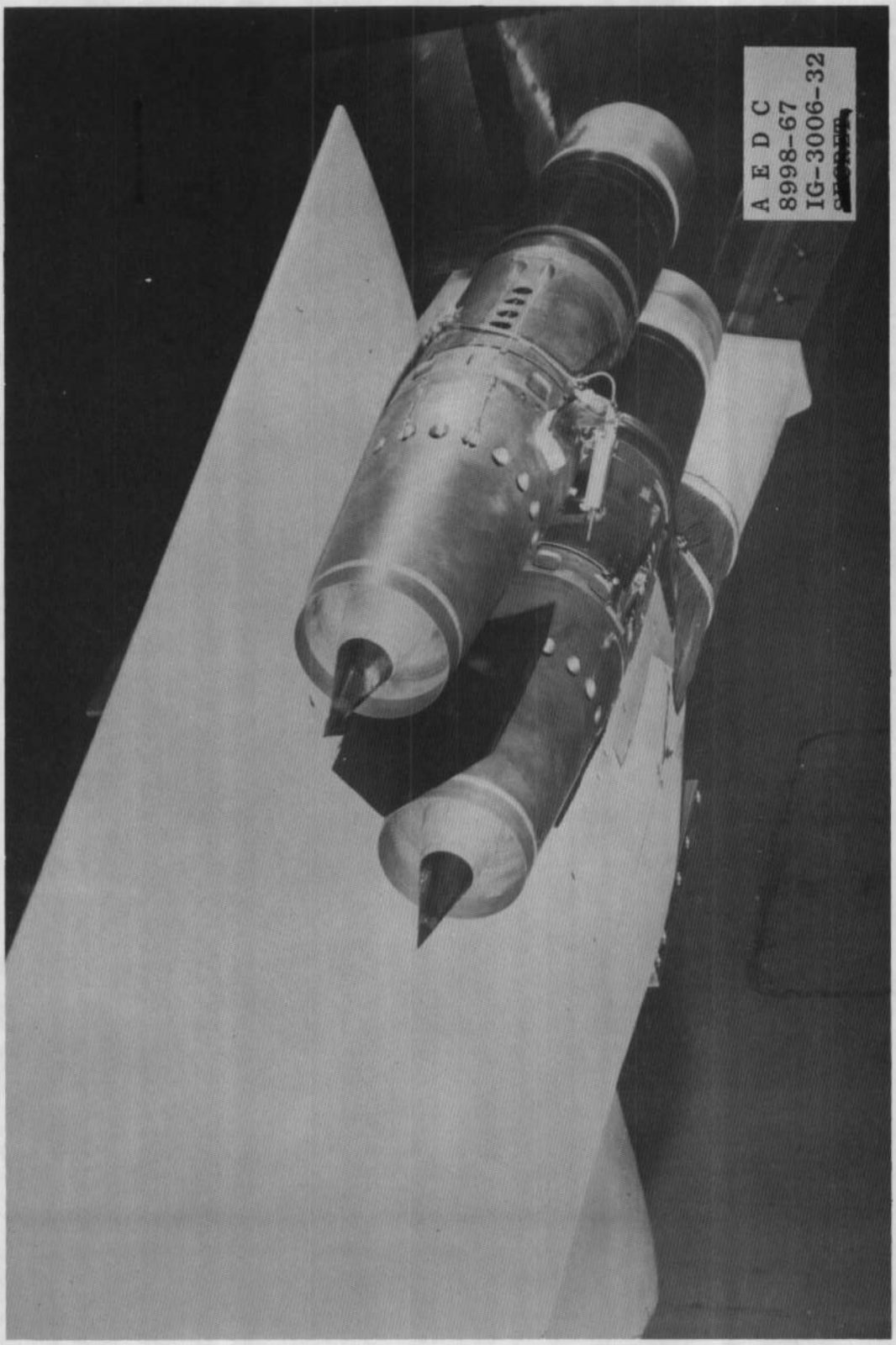

b. Short Splitter Plate

Fig. 6 Continued

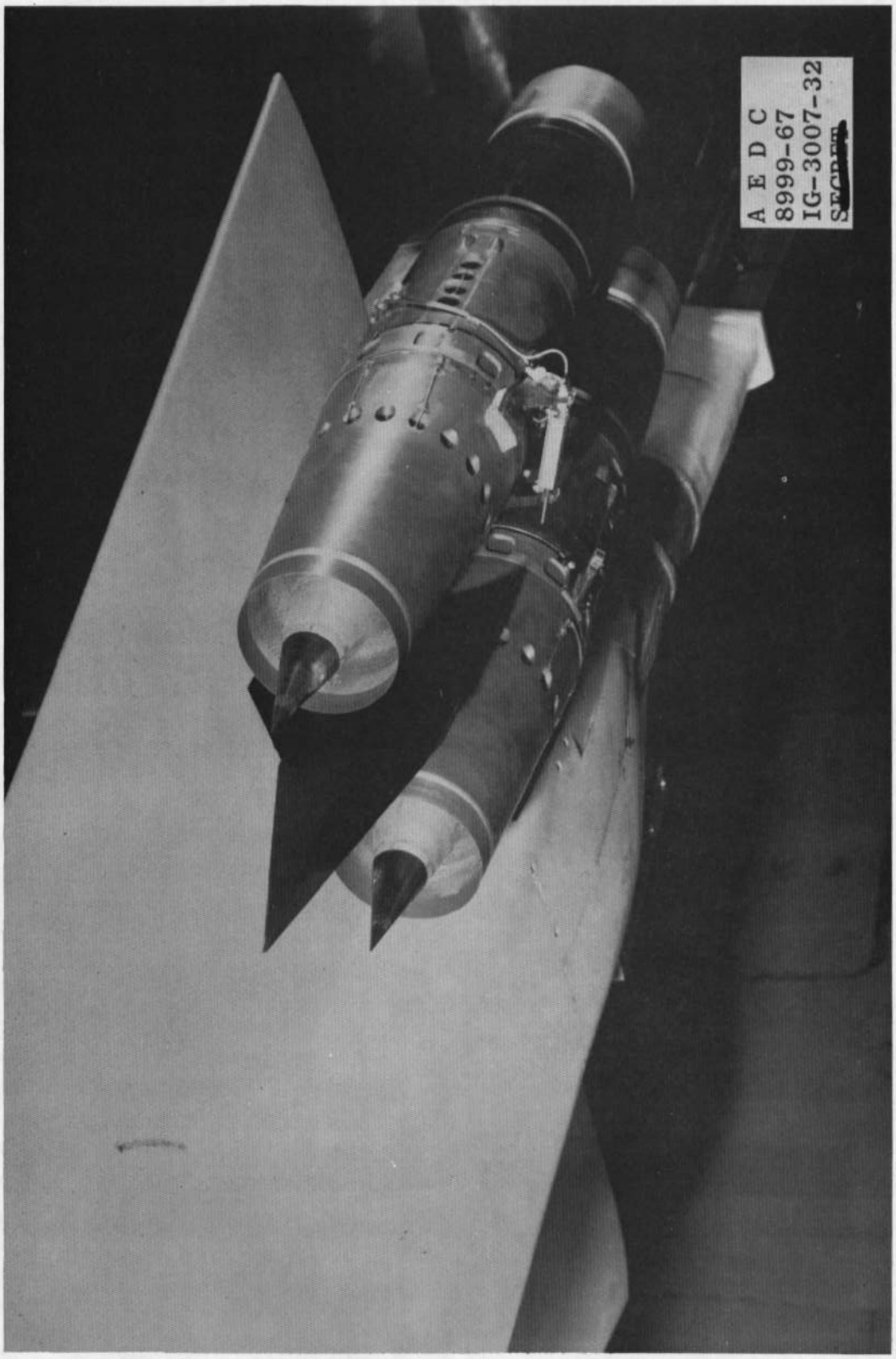

c. Long Splitter Plate

Fig. 6 Concluded

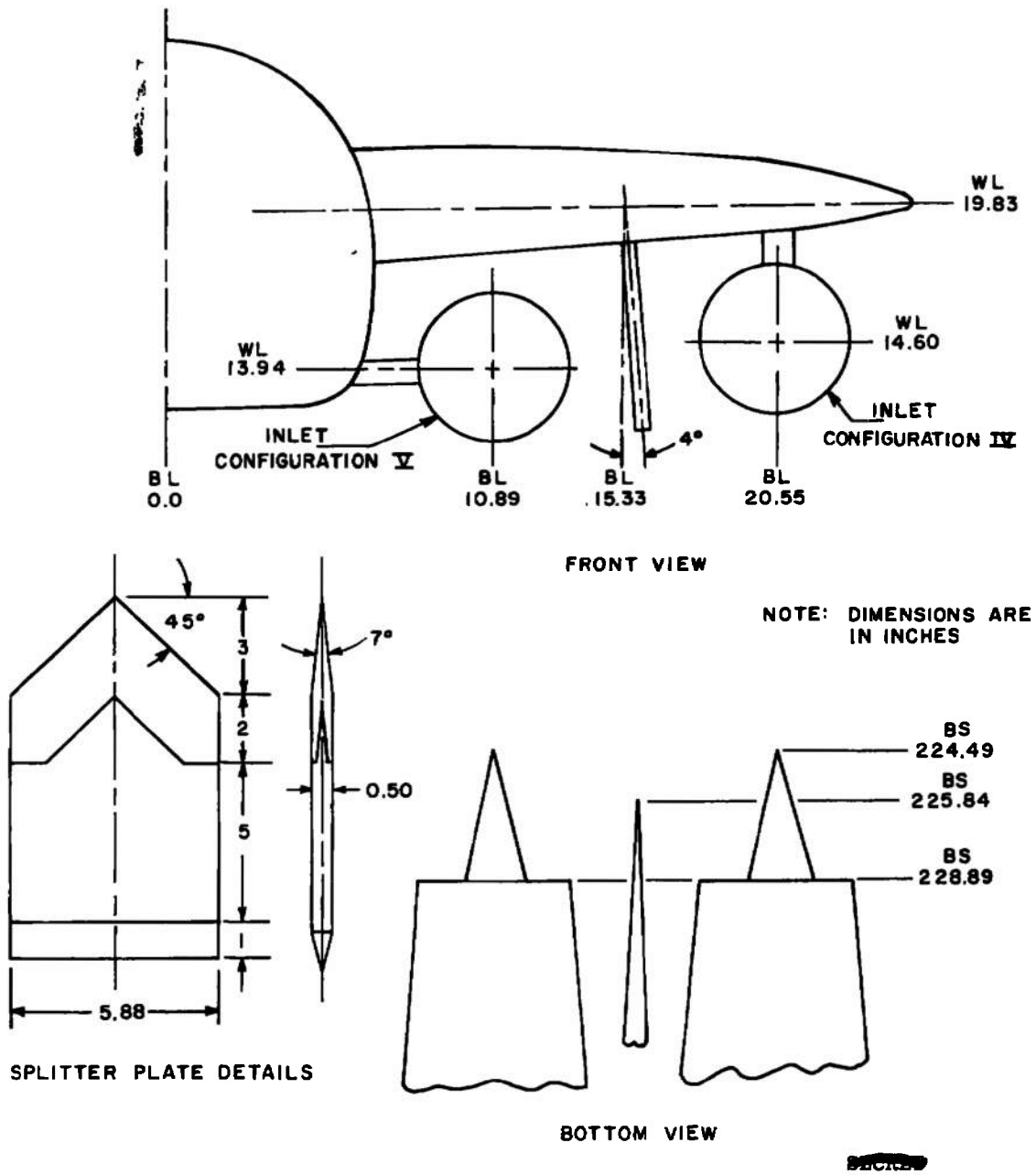

Fig. 7 Dimensioned Sketch of the Primary Inlet-Splitter Plate Configuration

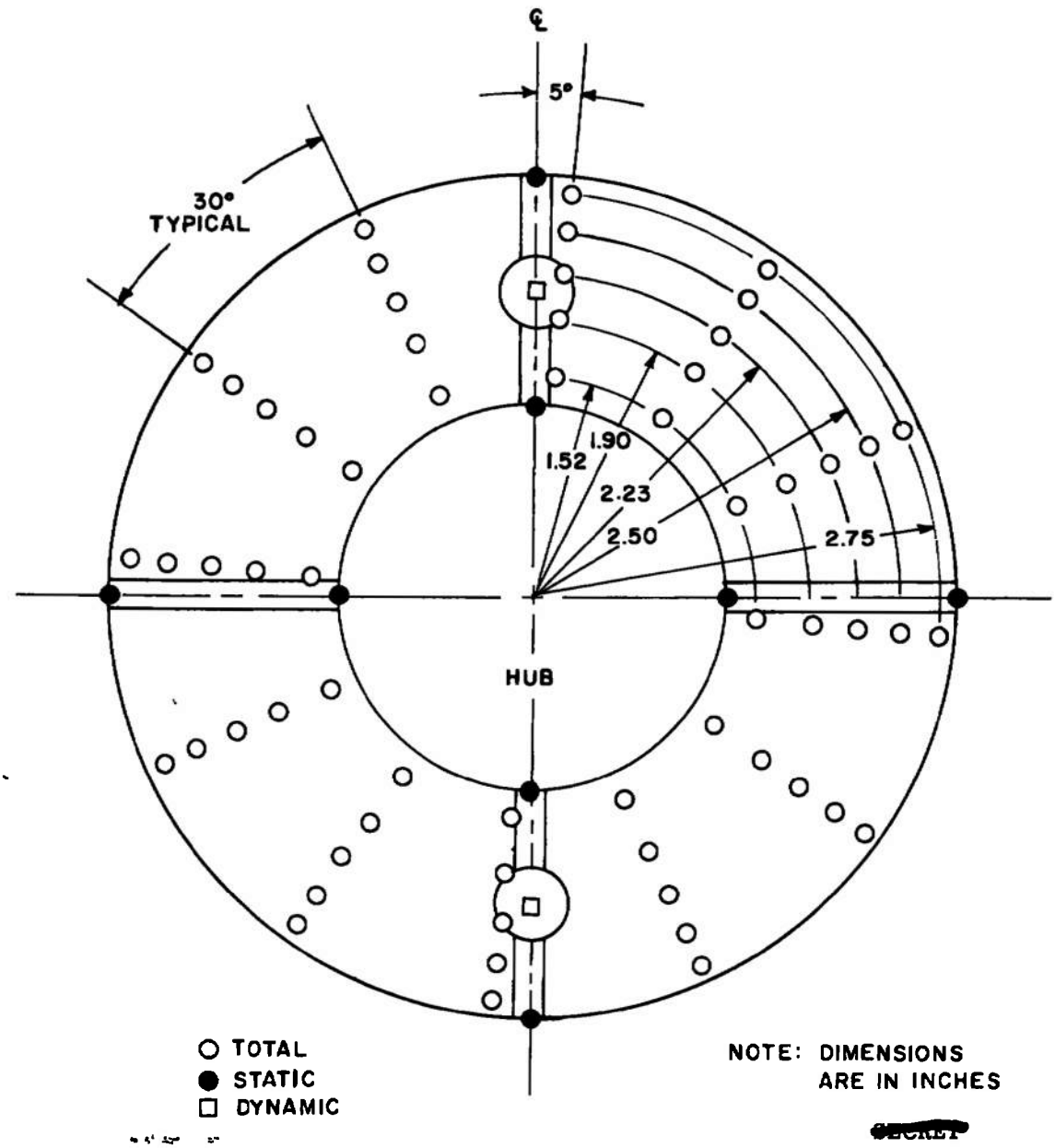

Fig. 8 Compressor-Face Instrumentation

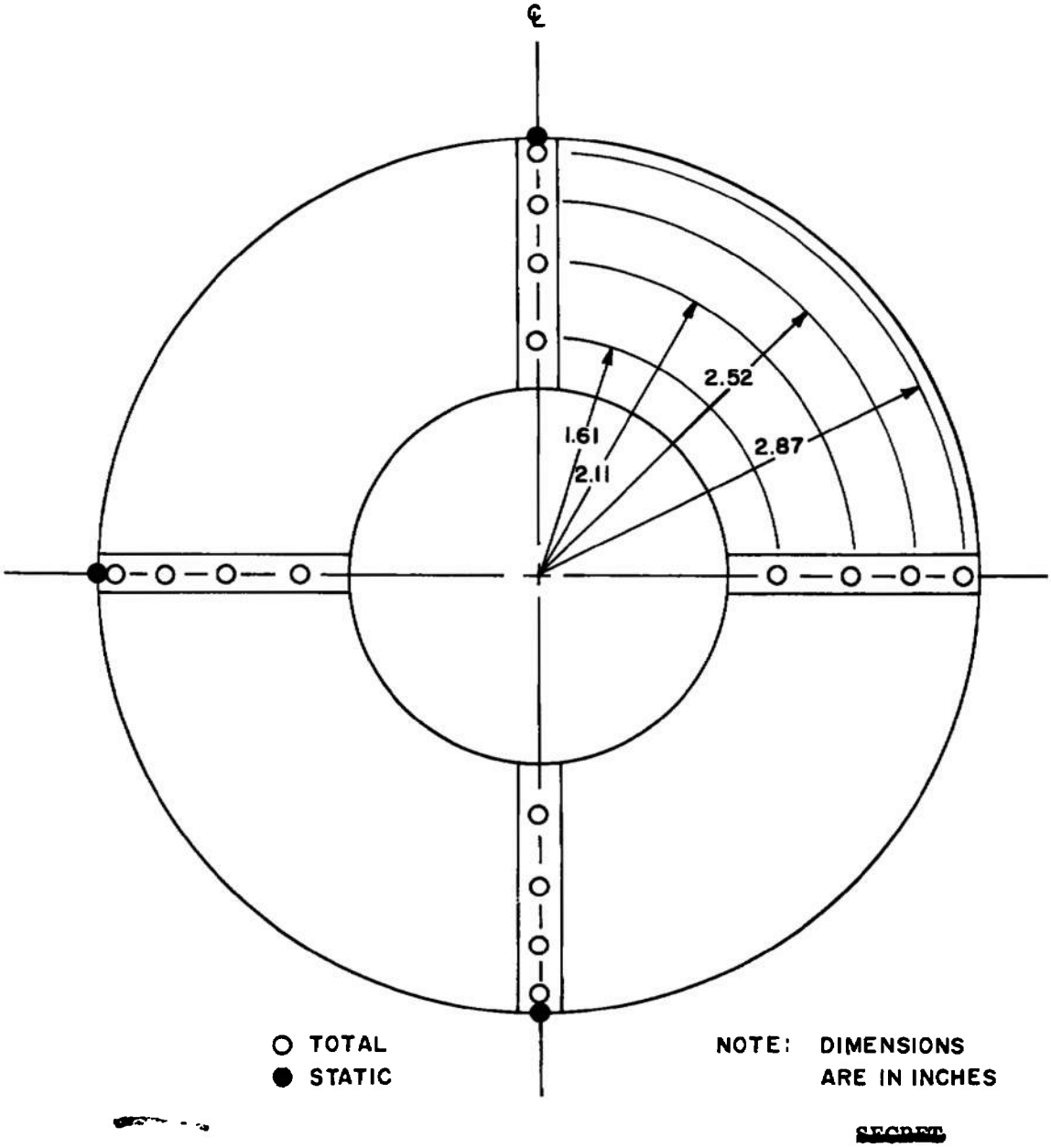

Fig. 9 Flow Tube Instrumentation

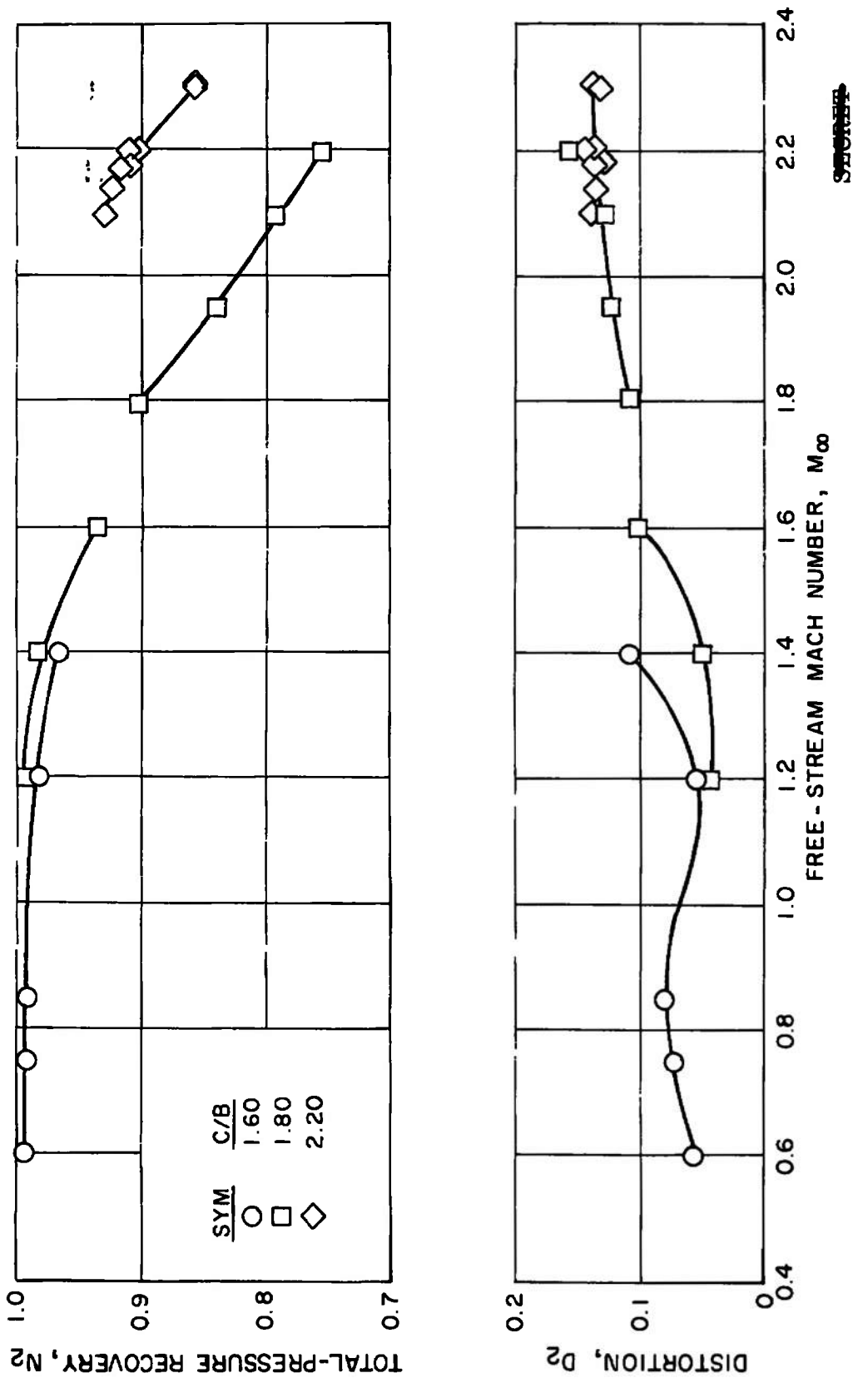

a. Inlet Location I

Fig. 10 Effect of Free-Stream Mach Number on Inlet Performance for Fixed-Geometry Centerbodies at Cruise Attitude

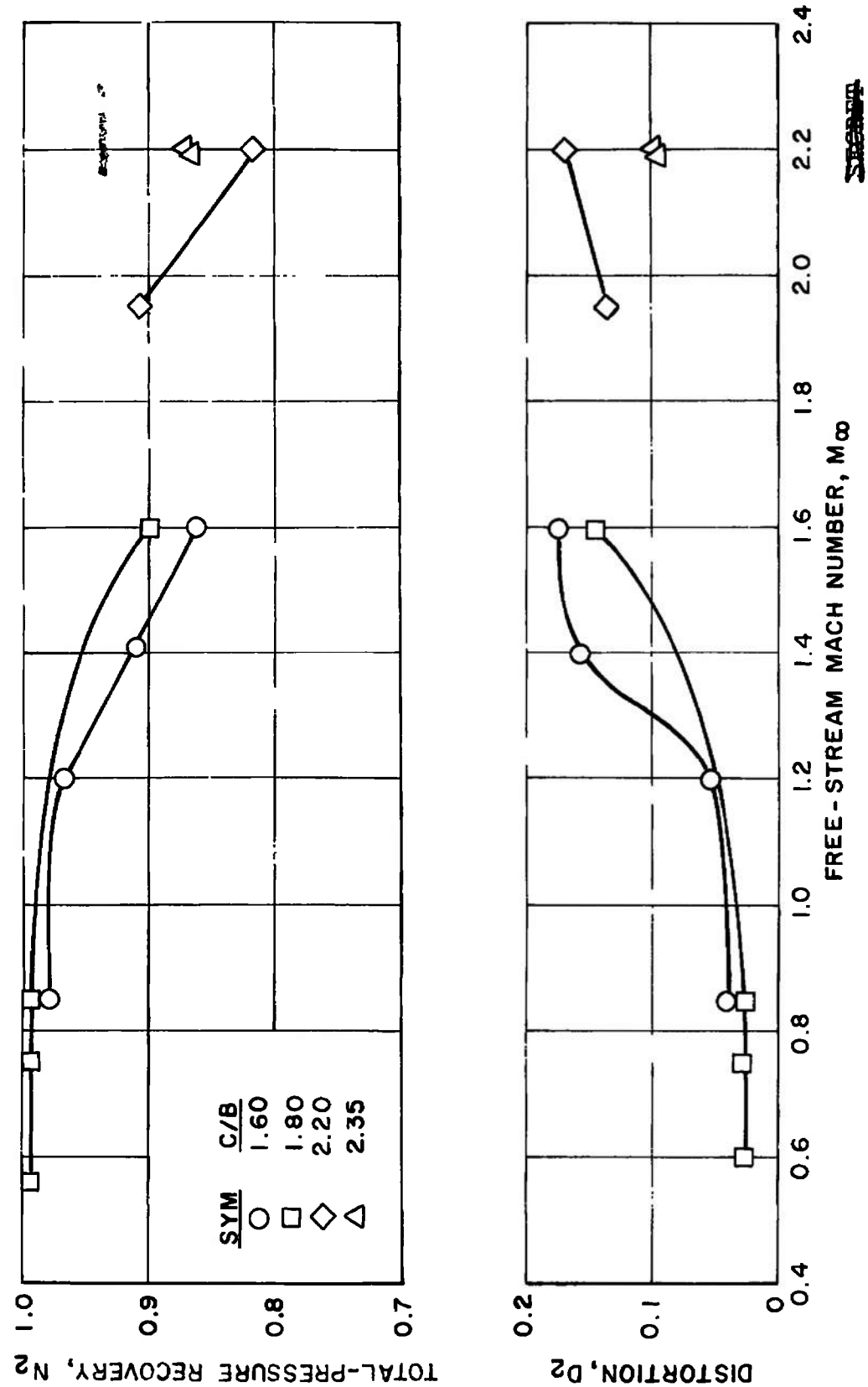

b. Inlet Location II

Fig. 10 Continued

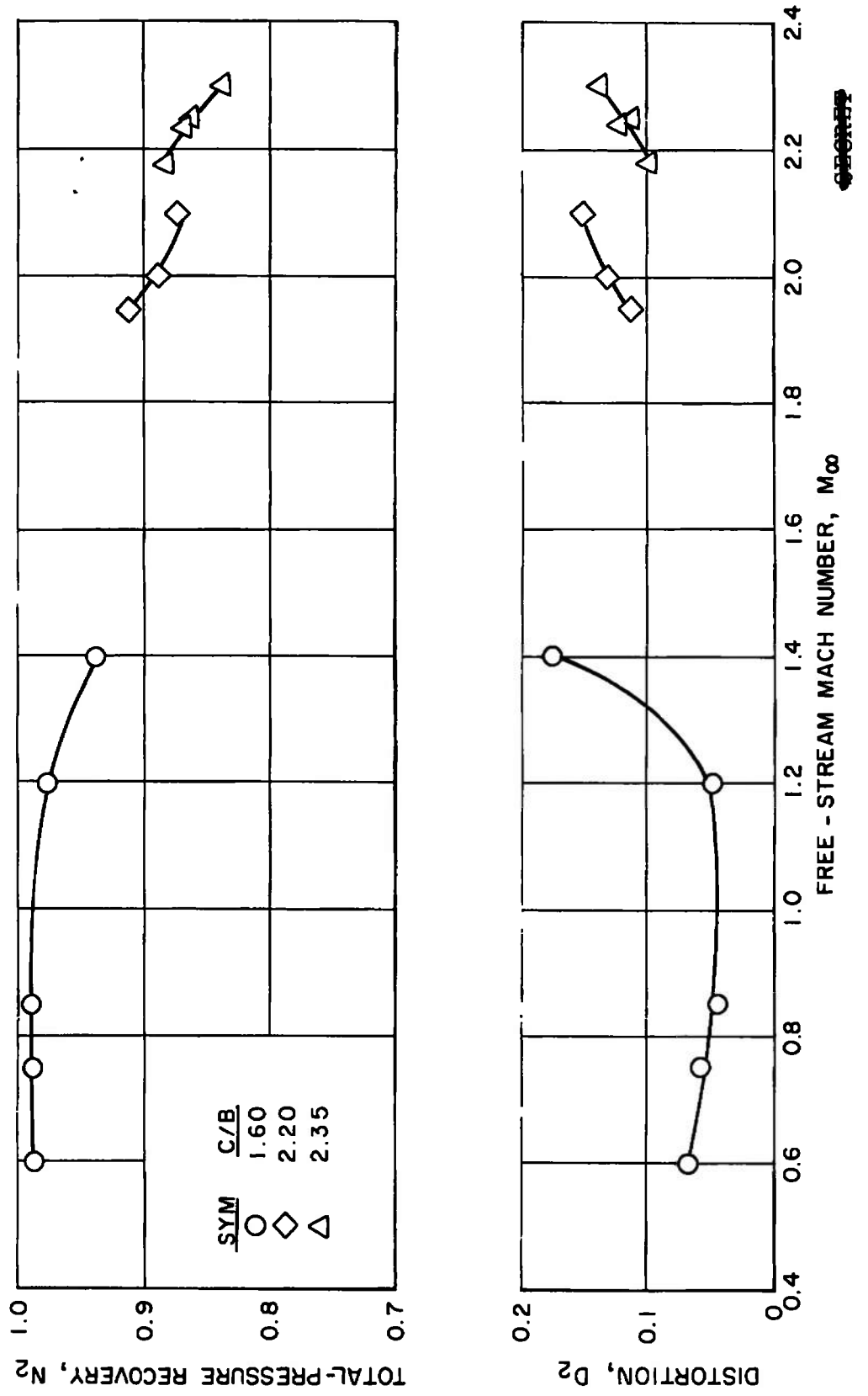

c. Inlet Location III

Fig. 10 Continued

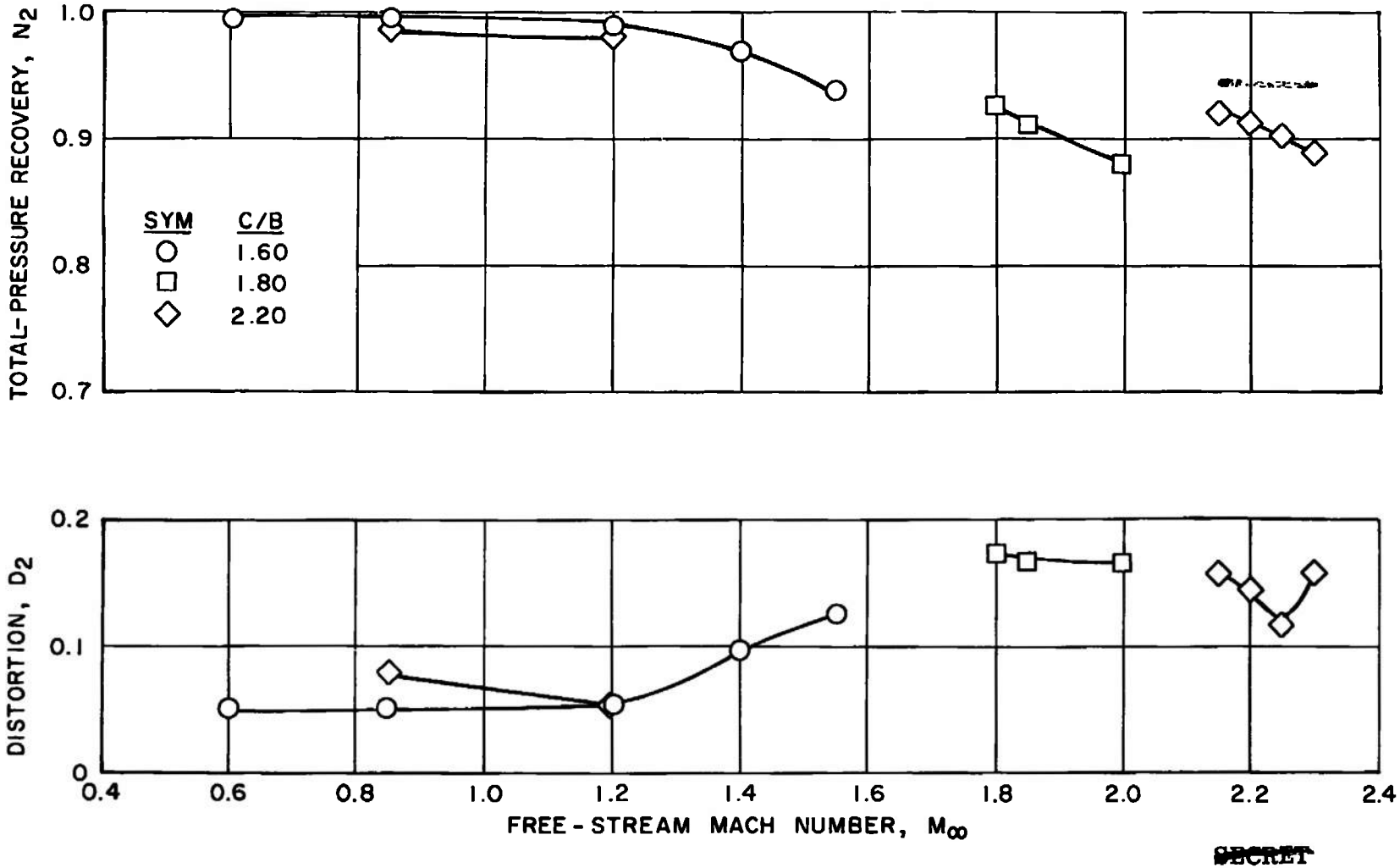

d. Inlet Location IV

Fig. 10 Continued

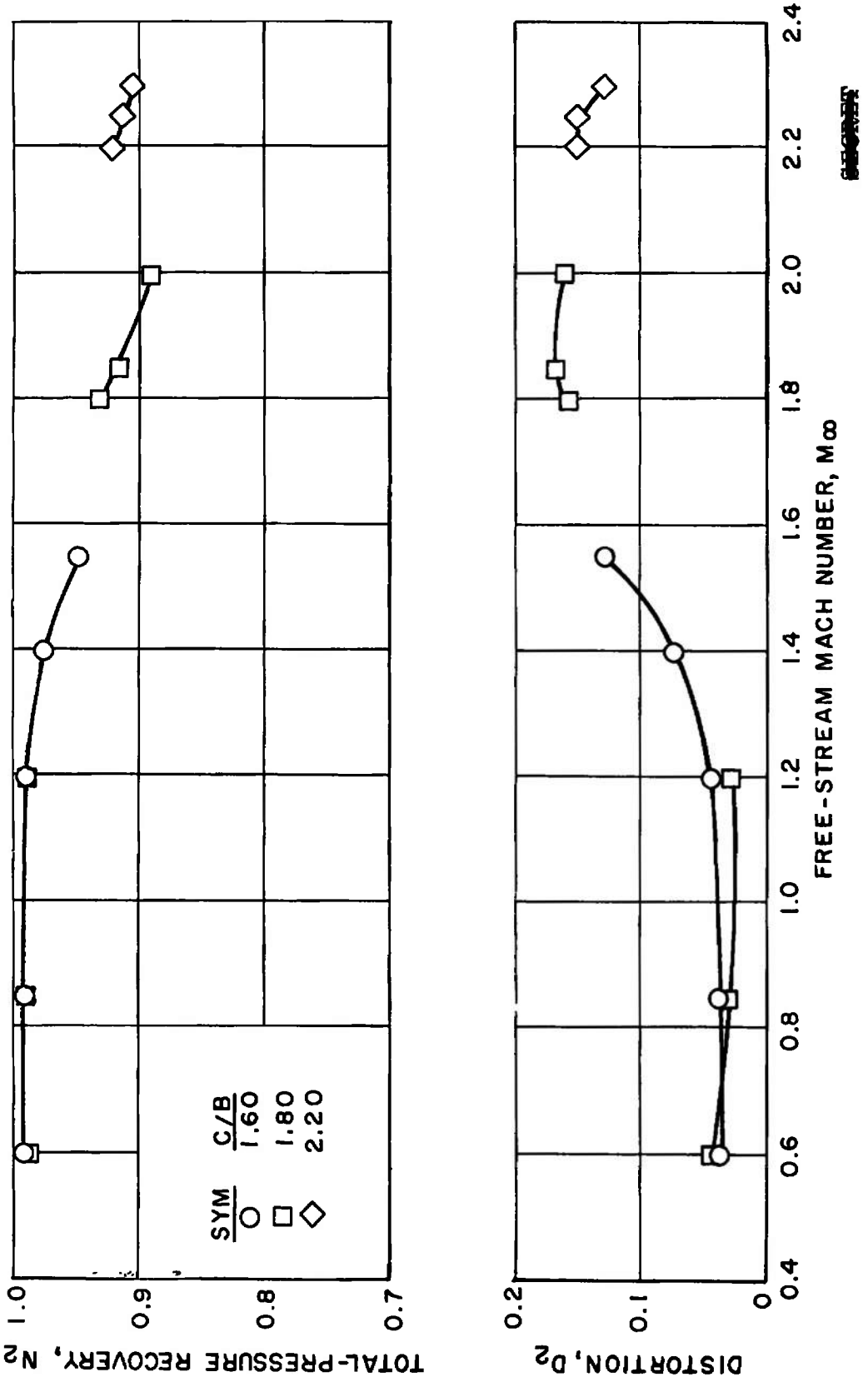

e. Inlet Location V

Fig. 10 Concluded

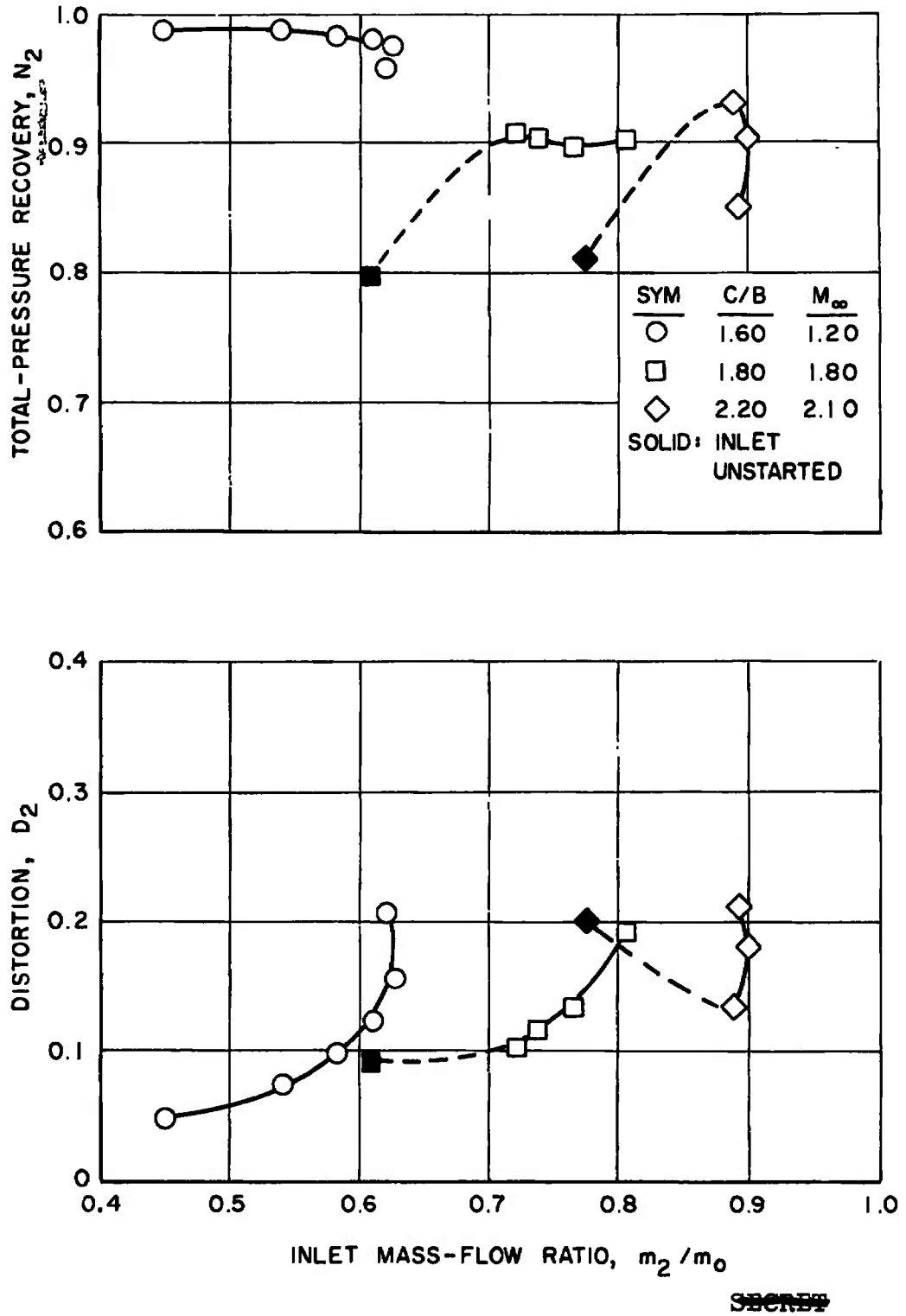

a. Inlet Location I

Fig. 11 Effect of Inlet Mass-Flow Ratio on Inlet Performance at Model Cruise Attitude

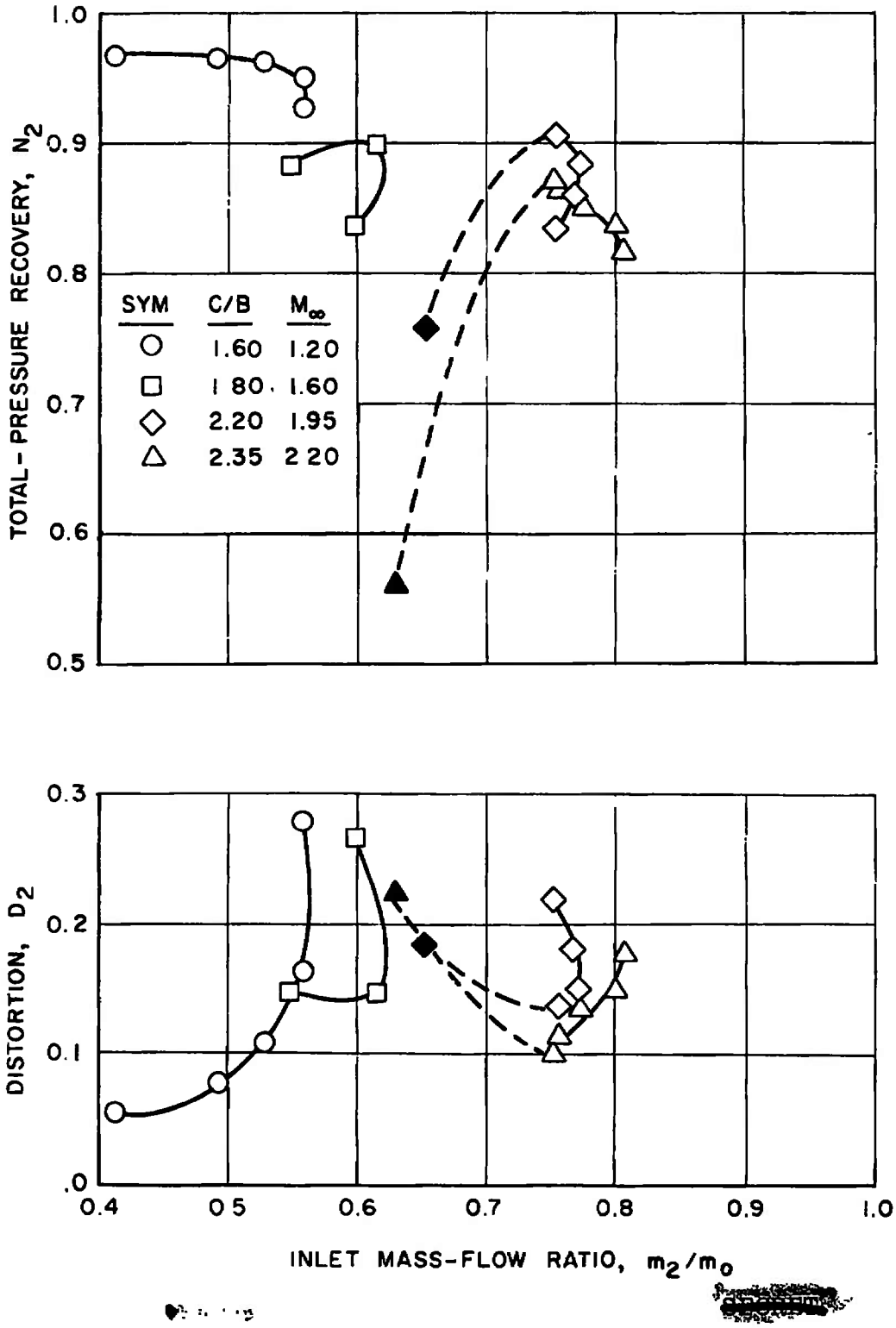

b. Inlet Location II

Fig. 11 Continued

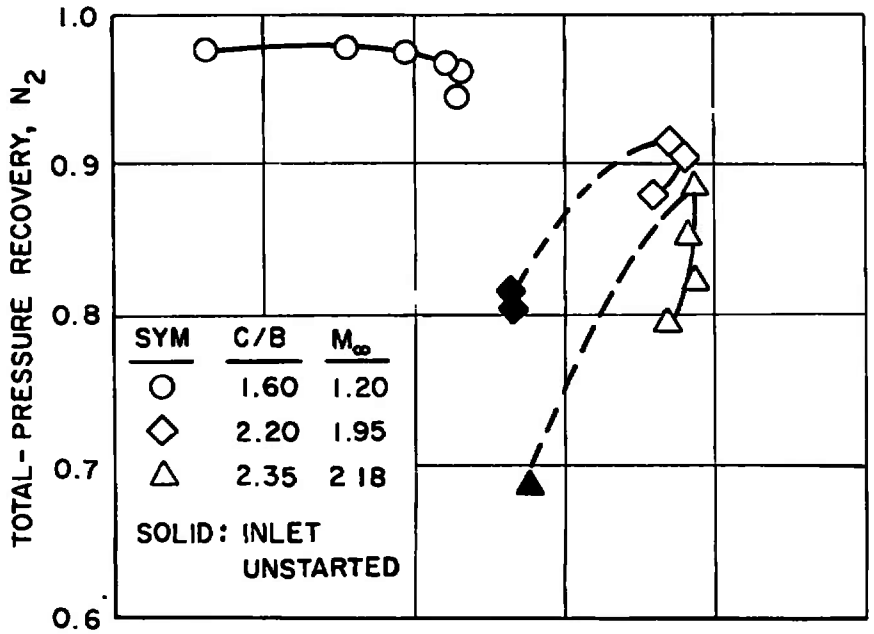

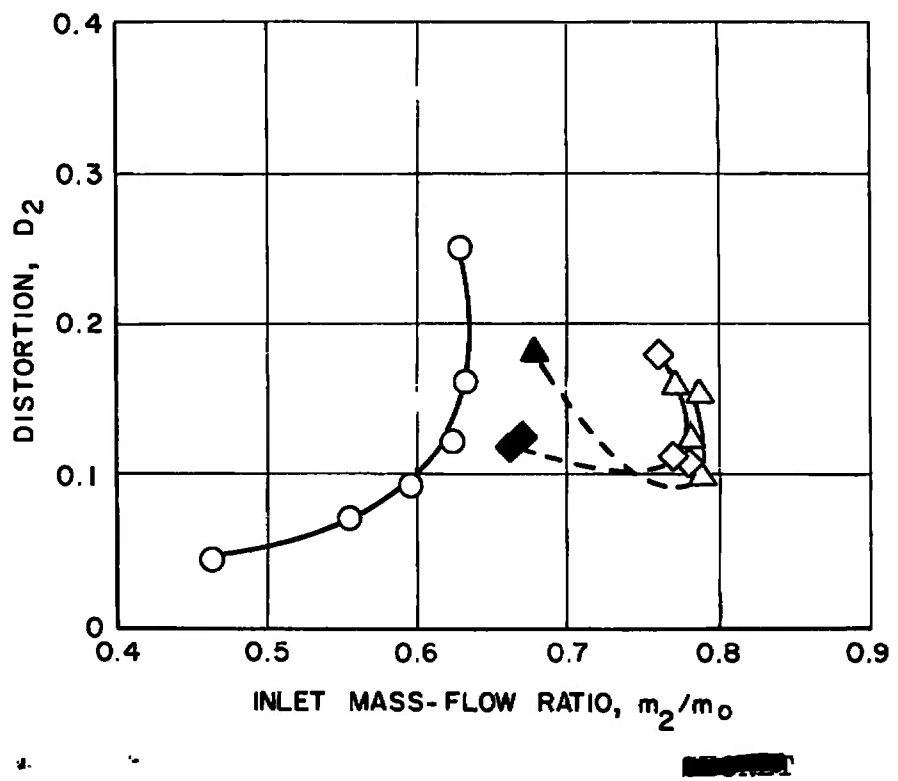

[redacted]

c. Inlet Location III

Fig. 11 Continued

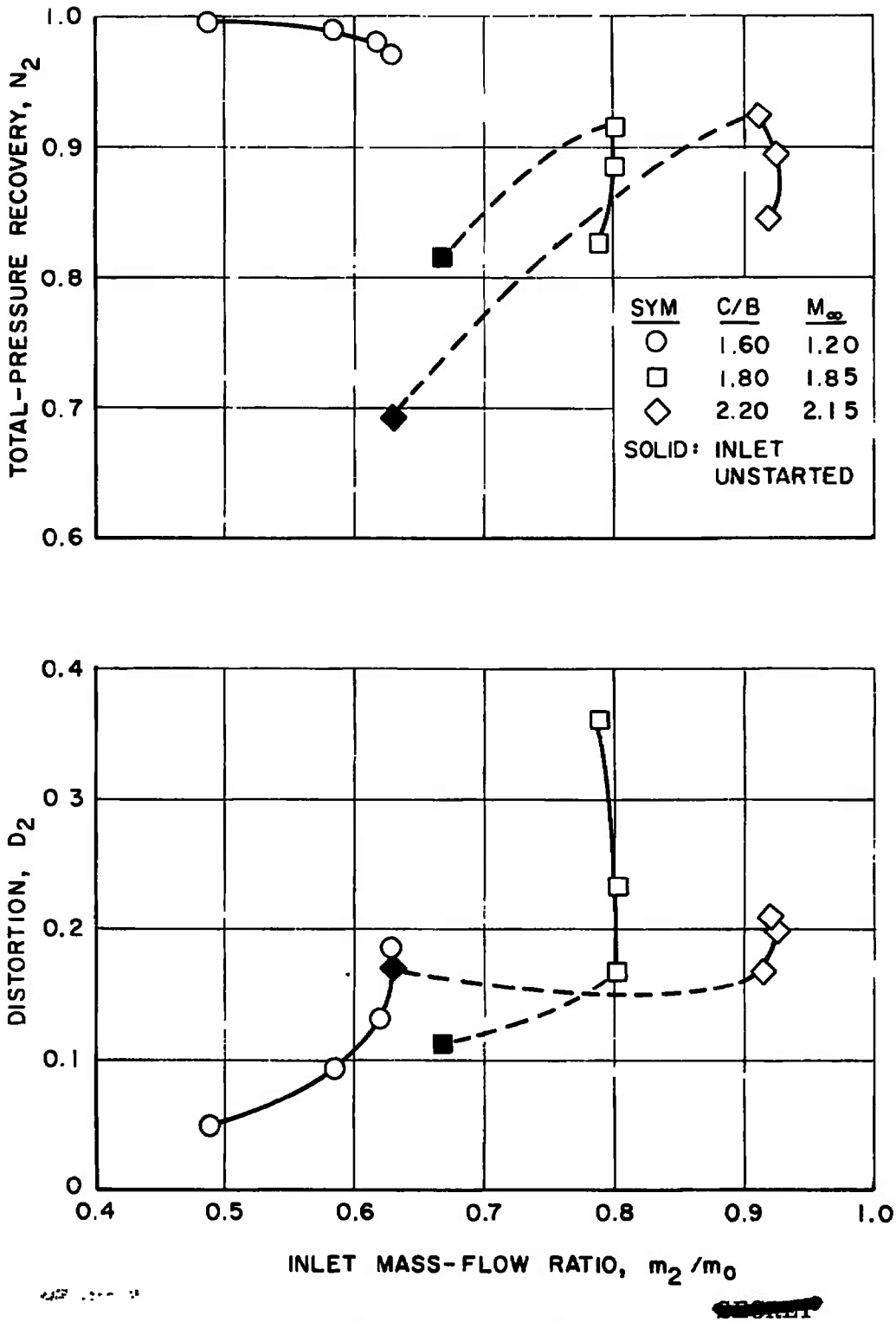

d. Inlet Location IV

Fig. 11 Continued

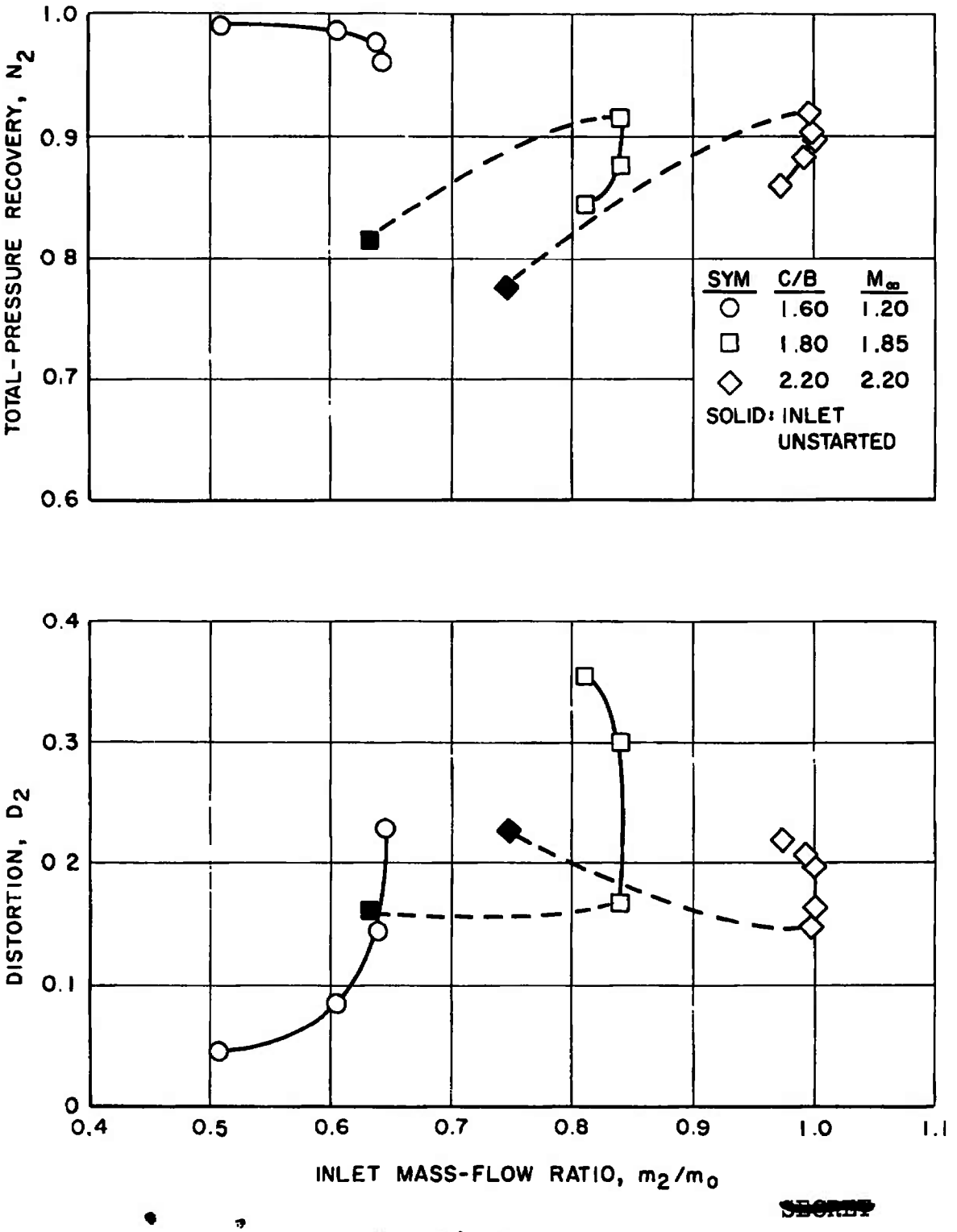

[redacted]

e. Inlet Location V

Fig. 11 Concluded

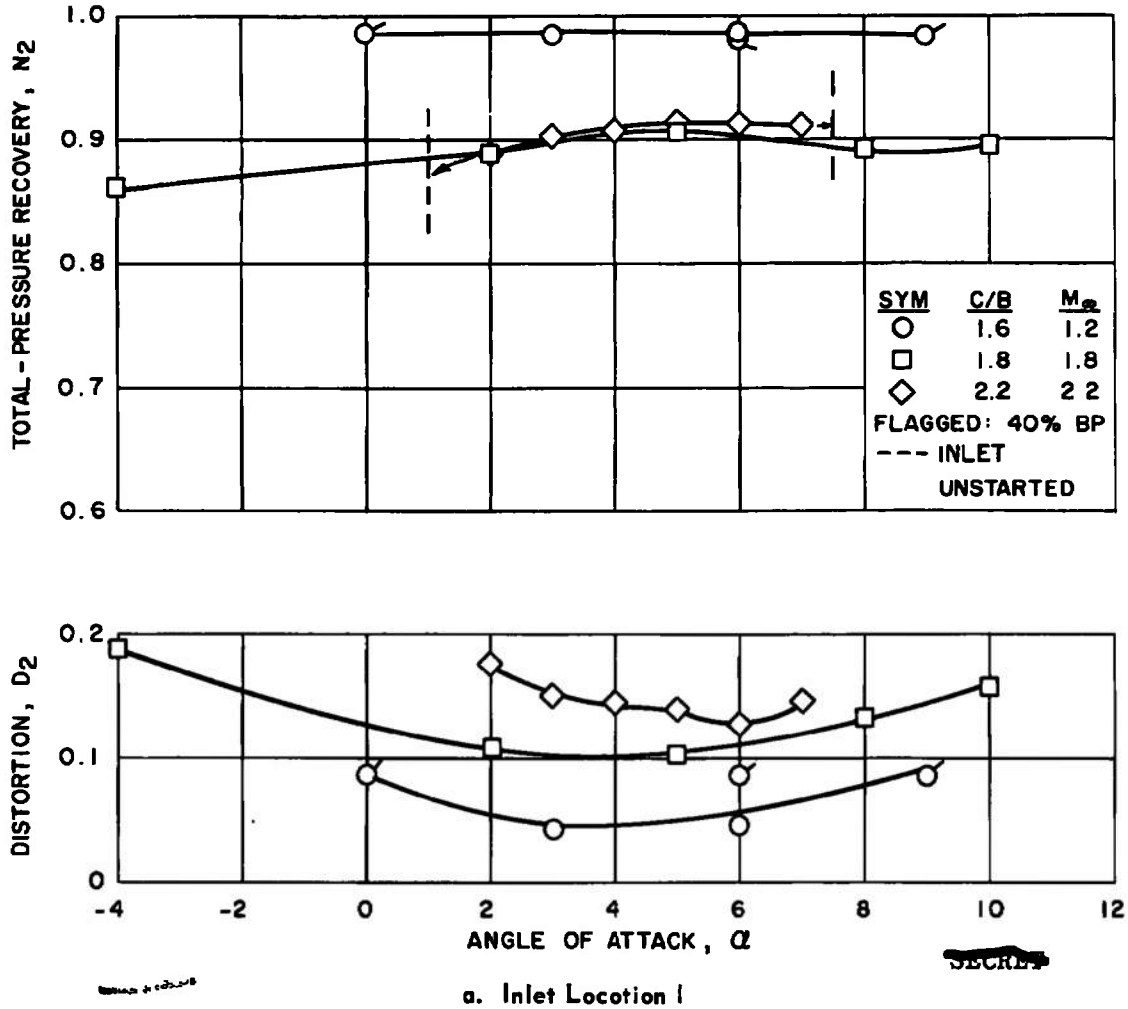

a. Inlet Locotion I

Fig. 12 Effect of Angle of Attack on Inlet Performance, ψ = 0

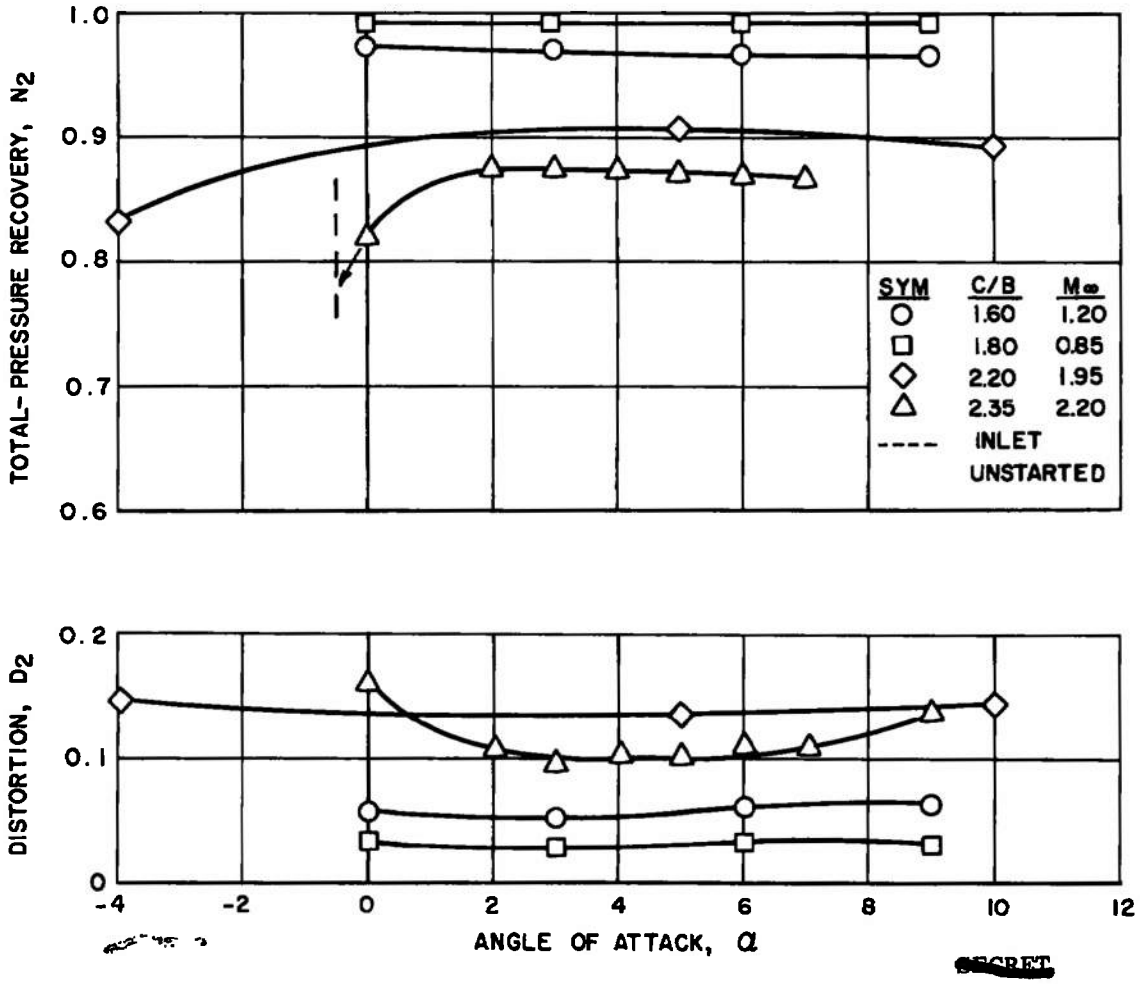

b. Inlet Location II

Fig. 12 Continued

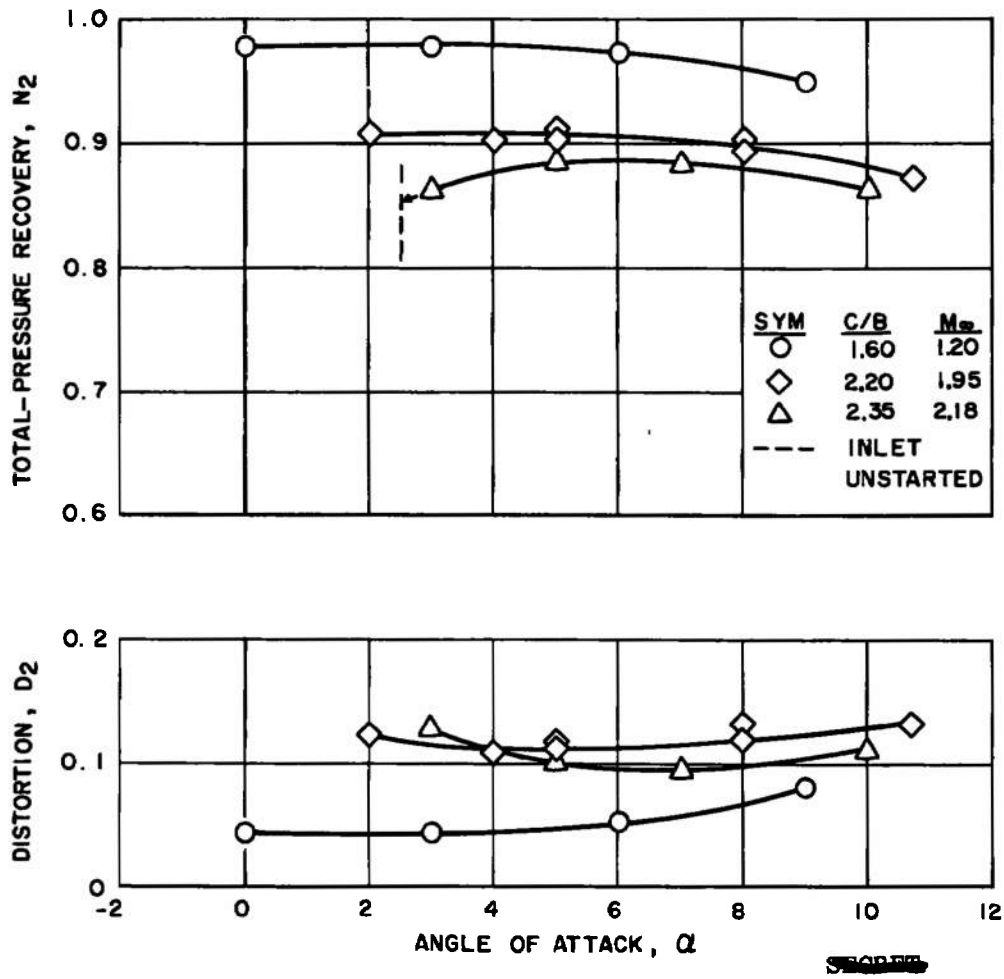

c. Inlet Location III

Fig. 12 Continued

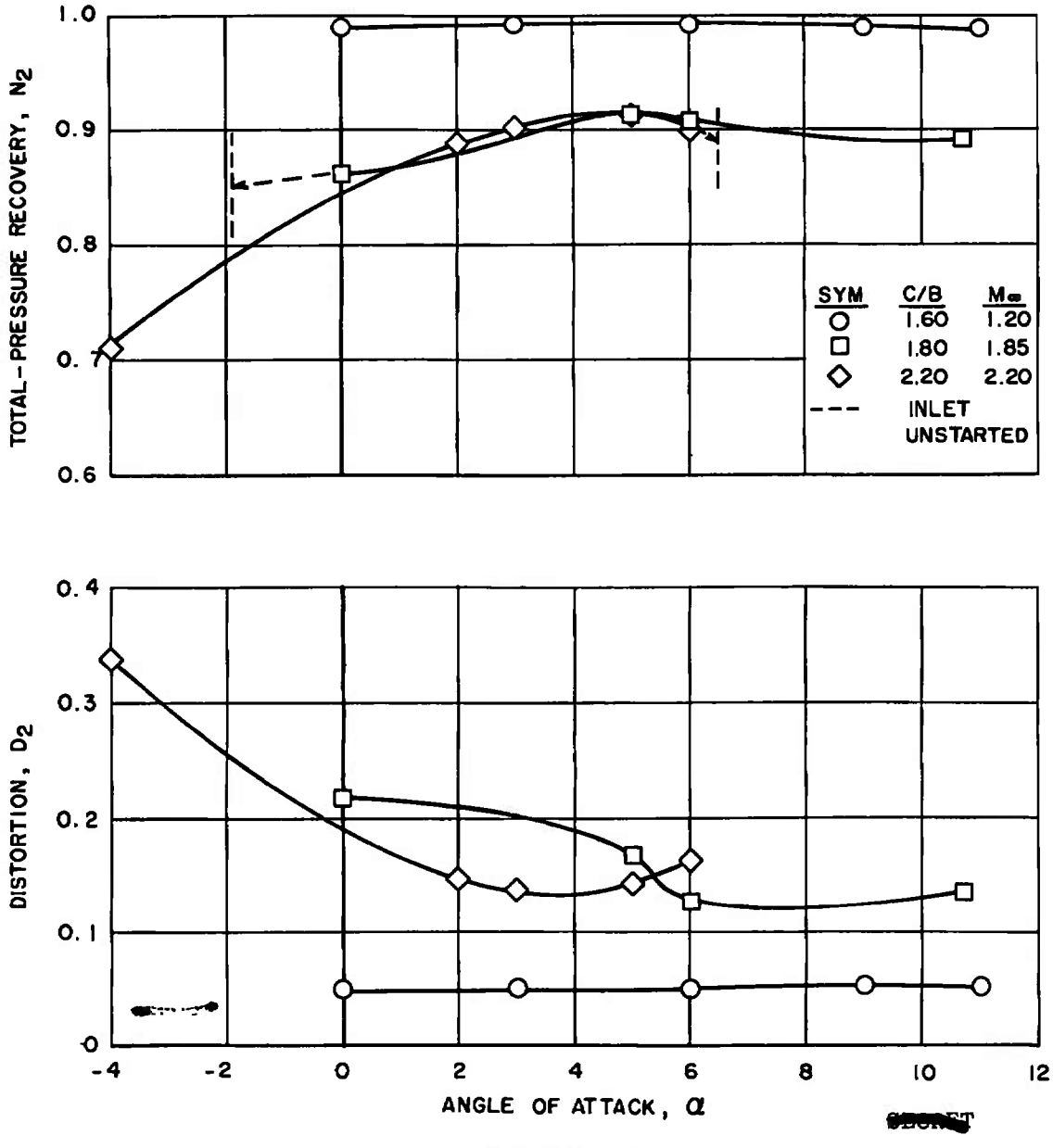

d. Inlet Location IV

Fig. 12 Continued

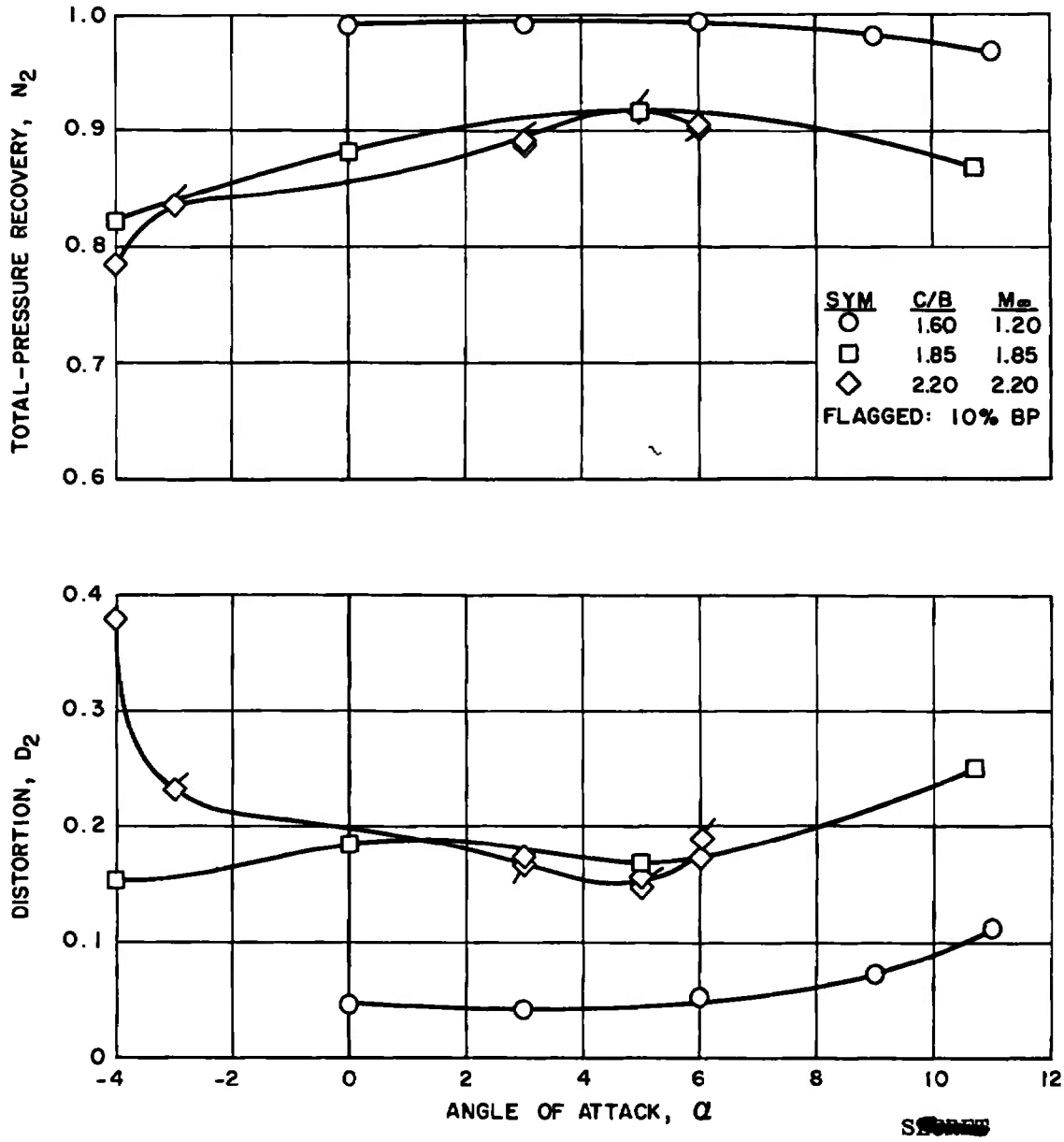

e. Inlet Location V

Fig. 12 Concluded

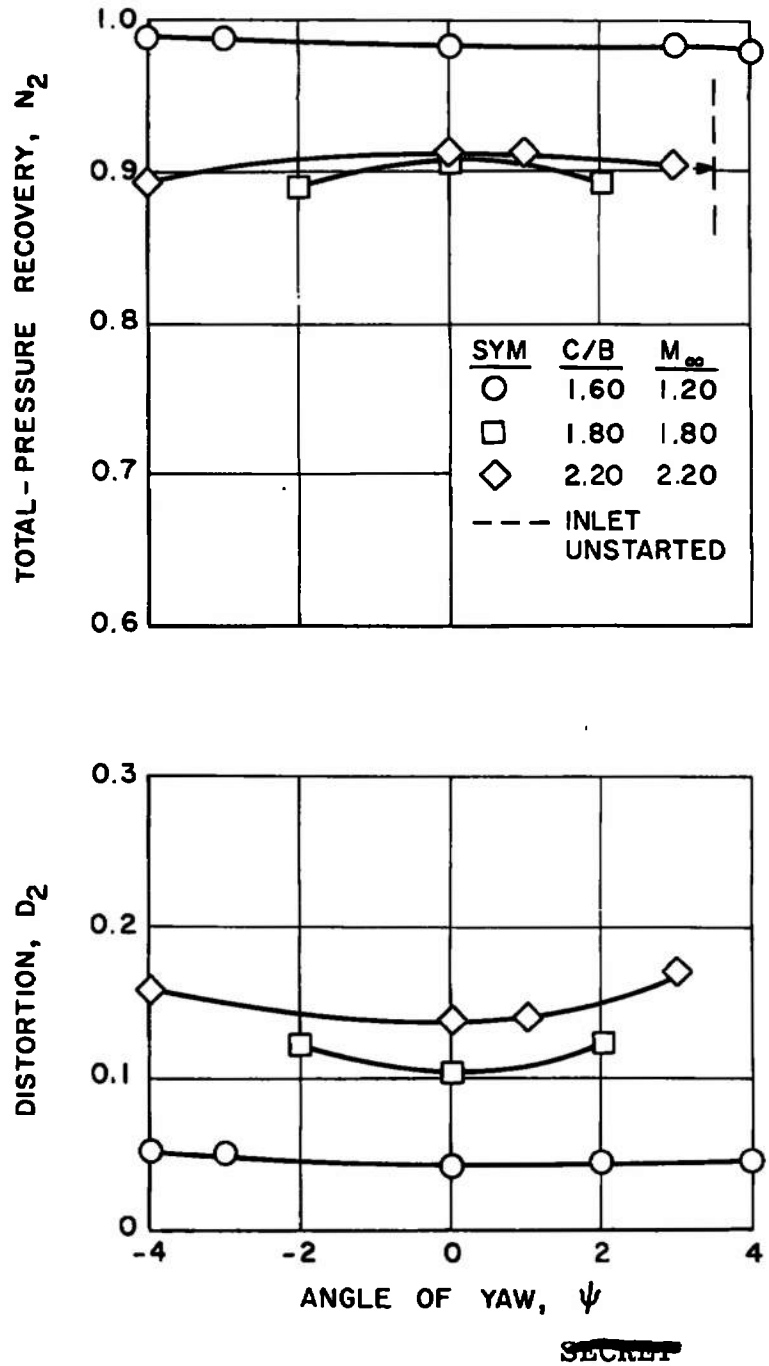

[redacted]

a. Inlet Location I

Fig. 13 Effect of Yaw Angle on Inlet Performance at Cruise Angle of Attack

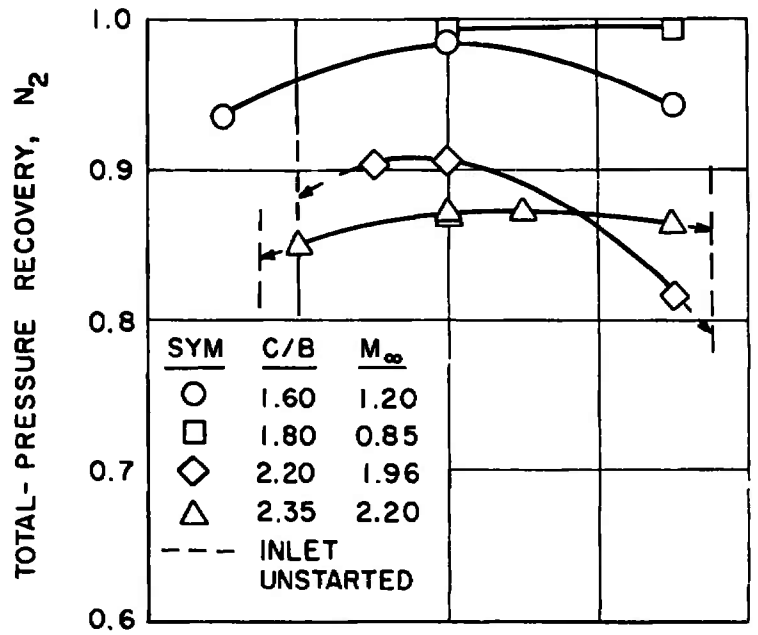

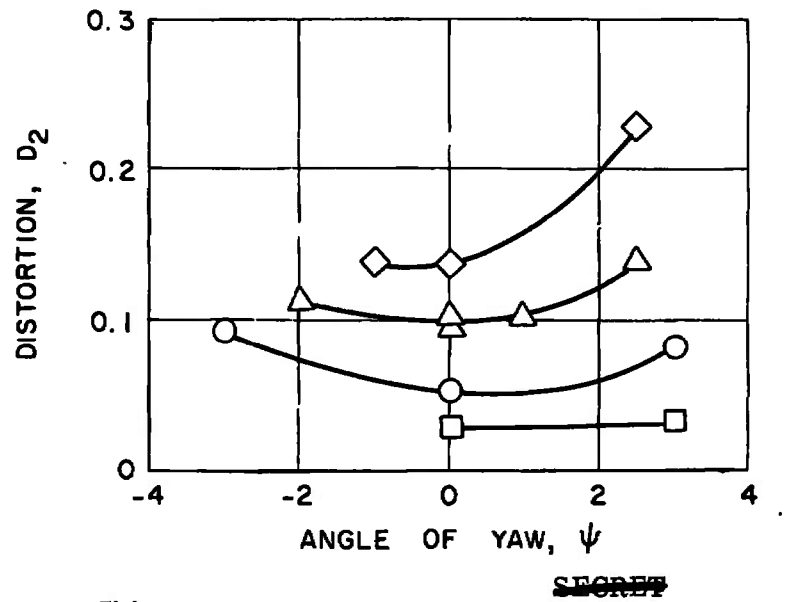

SECRET

b. Inlet Location II

Fig. 13 Continued

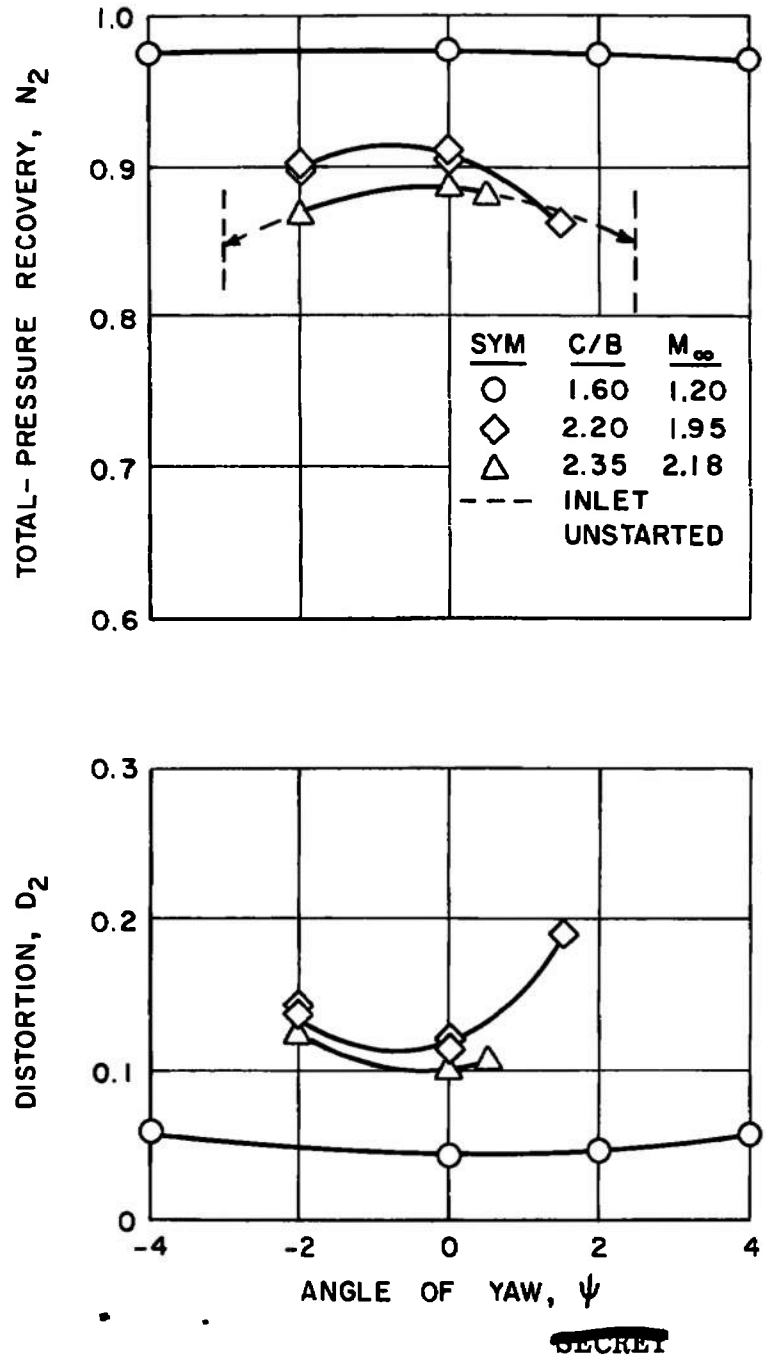

SECRET

c. Inlet Location III

Fig. 13 Continued

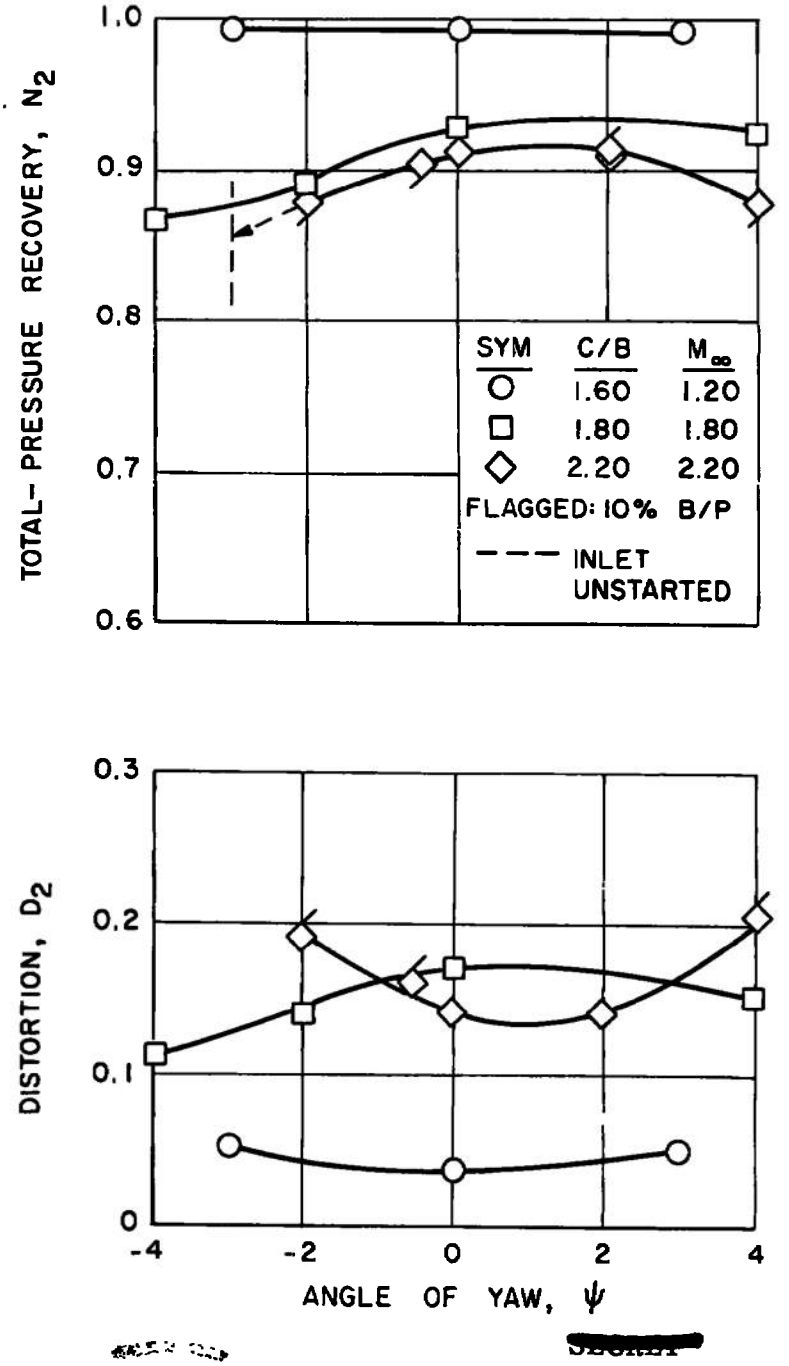

d. Inlet Location IV

Fig. 13 Continued

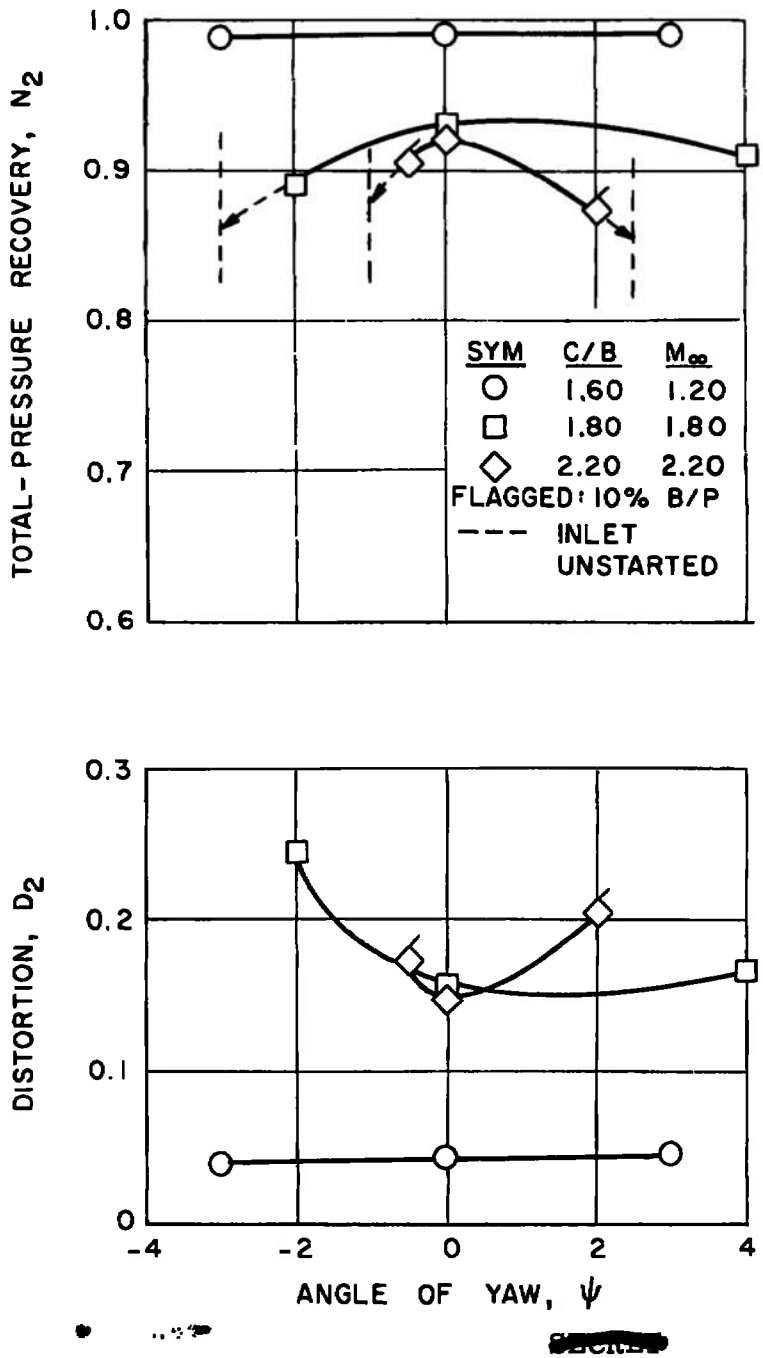

e. Inlet Location V

Fig. 13 Concluded

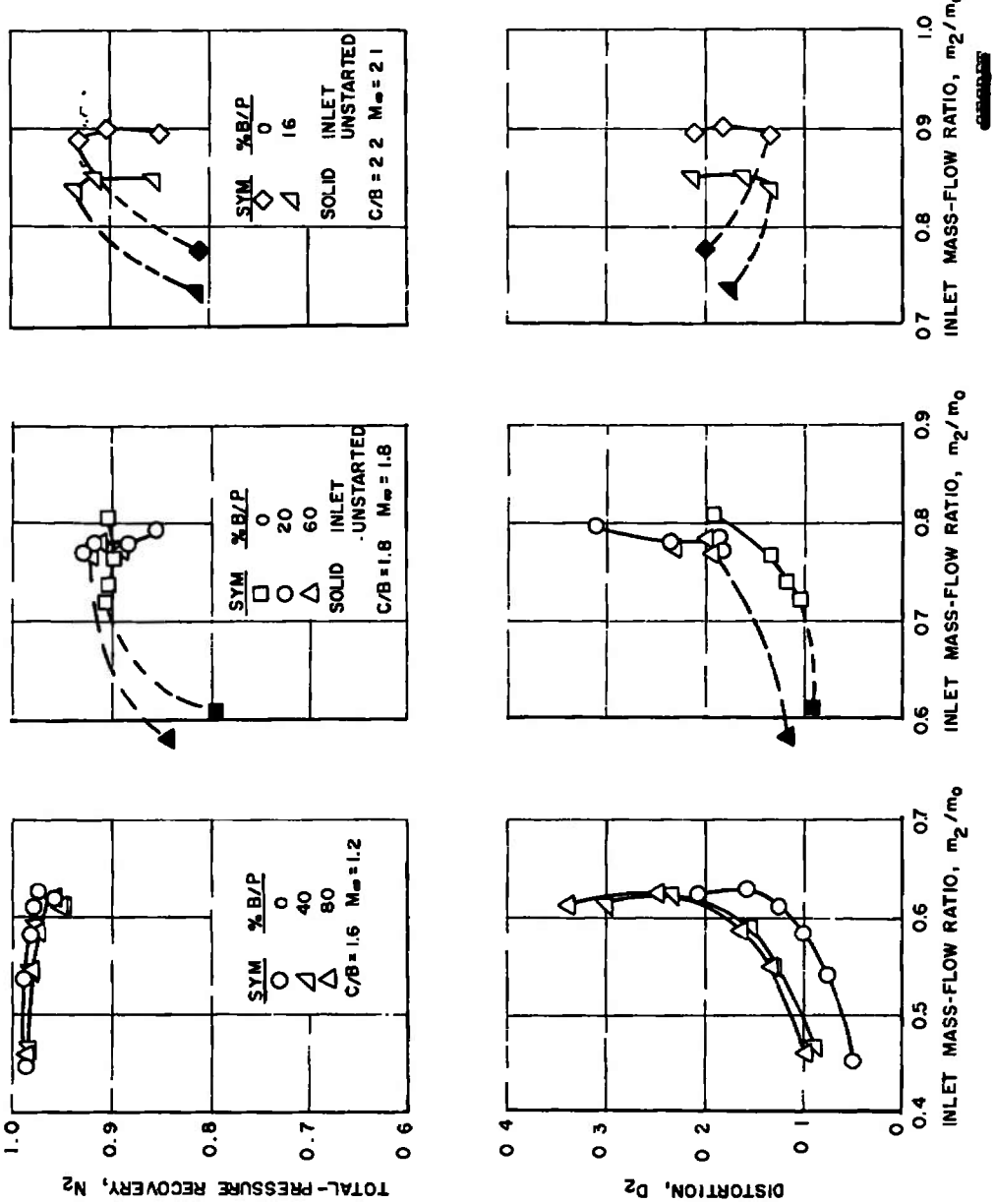

a. Inlet Location I

Fig. 14 Effect of Bypass Opening on Inlet Performance at Model Cruise Attitude

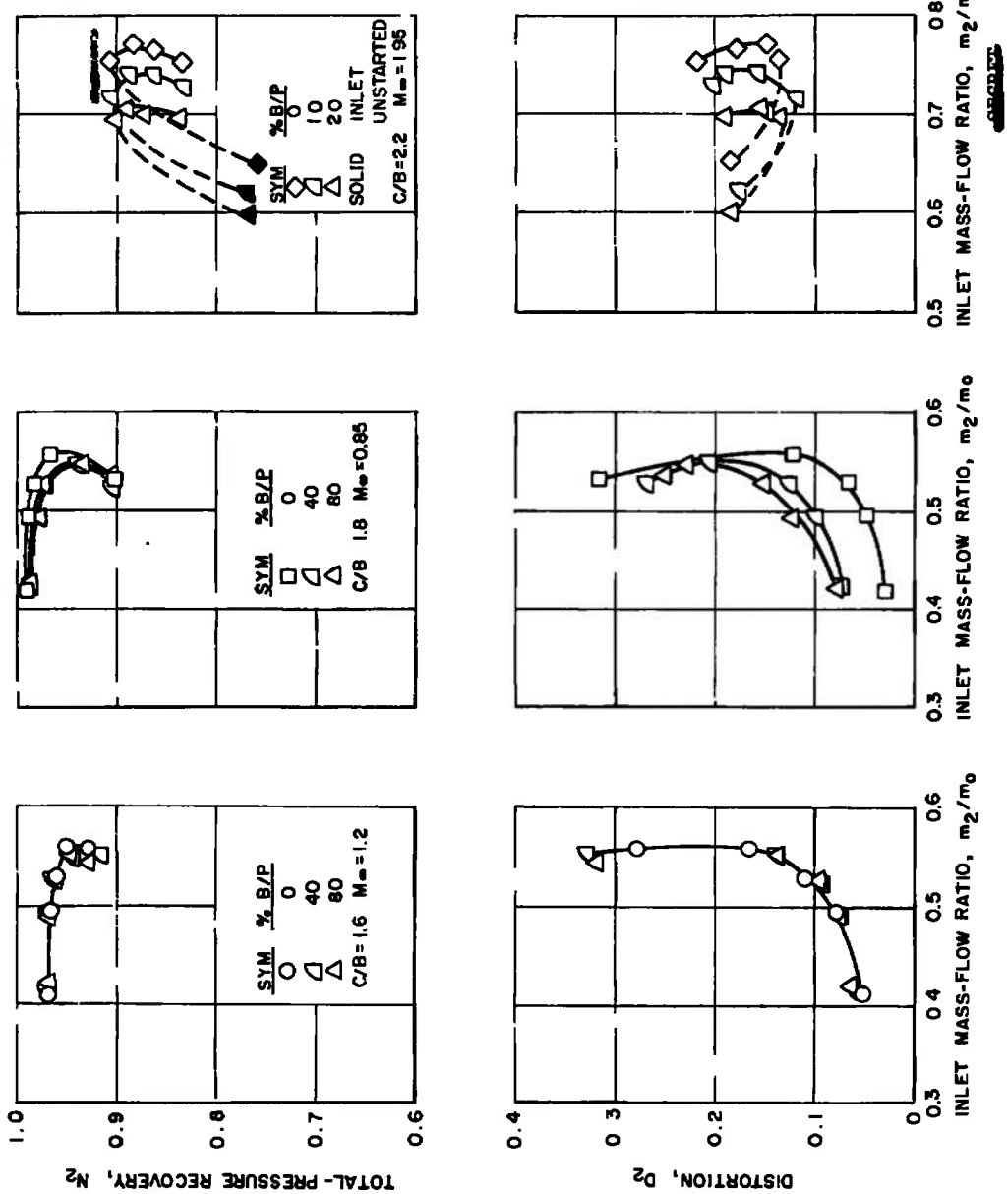

b. Inlet Location II

Fig. 14 Continued

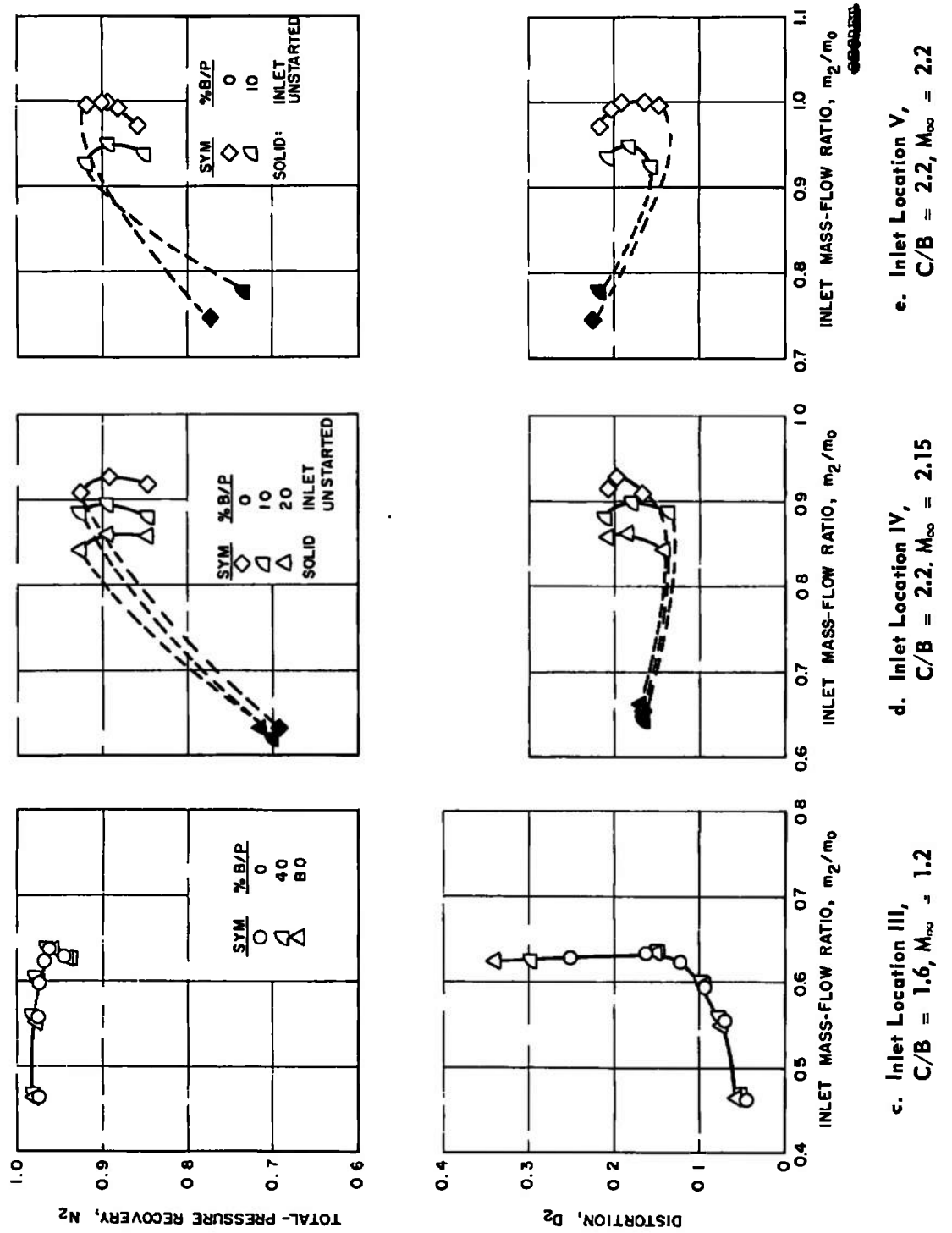

c. Inlet Location III, C/B = 1.6, M_∞ = 1.2

d. Inlet Location IV, C/B = 2.2, M_∞ = 2.15

e. Inlet Location V, C/B = 2.2, M_∞ = 2.2

Fig. 14 Concluded

The reverse side of this page is blank.

DOCUMENT CONTROL DATA - R&D

(Security classification of title, body of abstract and indexing annotation must be entered when the overall report is classified)

1. ORIGINATING ACTIVITY *(Corporate author)*
Arnold Engineering Development Center
ARO, Inc., Operating Contractor
Arnold Air Force Station, Tennessee

2a. REPORT SECURITY CLASSIFICATION
[redacted]

2b. GROUP
[redacted]

3. REPORT TITLE
WIND TUNNEL INVESTIGATION OF A 1/9-SCALE BOEING COMPANY AMSA AIRPLANE-INLET MODEL AT TRANSONIC AND SUPERSONIC MACH NUMBERS (U)

4. DESCRIPTIVE NOTES *(Type of report and inclusive dates)*
June 19 to August 4, 1967 - Final Report

5. AUTHOR(S) *(First name, middle initial, last name)*
D. C. Baker, ARO, Inc.

6. REPORT DATE	7a. TOTAL NO. OF PAGES	7b. NO. OF REFS
November 1967	61	1

8a. CONTRACT OR GRANT NO.	9a. ORIGINATOR'S REPORT NUMBER(S)
AF40(600)-1200	AEDC-TR-67-231
b. PROJECT NO. 139A	
c. Program Element 6340683F	9b. OTHER REPORT NO(S) *(Any other numbers that may be assigned this report)*
d.	N/A

10. DISTRIBUTION STATEMENT
Subject to special export controls; transmittal to foreign governments or foreign nationals requires approval of ASD (ASZD), Wright-Patterson AFB, Ohio. In addition to security requirements which apply to this document and must be met, each transmittal*

11. SUPPLEMENTARY NOTES	12. SPONSORING MILITARY ACTIVITY
Available in DDC	Aeronautical Systems Division (ASZD) Air Force Systems Command Wright-Patterson AFB, Ohio

13 ABSTRACT

Test results are presented for a 1/9-scale inlet model of the Boeing Company AMSA air induction system at transonic and supersonic free-stream Mach numbers. Inlet performance was determined for various inlet locations and is presented as a function of free-stream Mach number, inlet mass-flow ratio, angle of attack, angle of yaw, and bypass flow rate. (U)

This document is subject to special export controls and each transmittal to foreign governments or foreign nationals may be made only with prior approval of ASD (ASZD), Wright-Patterson AFB, Ohio.

Each transmittal of this document outside the Department of Defense must have prior approval of ASD (ASZD), Wright-Patterson AFB, Ohio

Distribution limited to U. S. Government Agencies only; Test and Evaluation; Nov. 72. Other requests for this document must be referred to Commander, Aeronautical Systems Div., Attn: YHT, Wright-Patterson AFB, Ohio 45433. Per TAB 72, dated 15 January, 1973.

* outside ASD (ASZD).

DD FORM 1 NOV 65 1473

14 KEY WORDS	LINK A		LINK B		LINK C	
	ROLE	WT	ROLE	WT	ROLE	WT
air induction system						
AMSA						
wind tunnel tests						
transonic flow						
supersonic flow						
performance						
Mach number effects						
mass-flow ratio effects						
angle-of-attack effects						
angle-of-yaw effects						
bypass flow rate effects						

1. Airplanes -- AMSA.
2. Advanced manned strategic aircraft
3. Air inlets -- Performance.

1 - 2.